

ALLERGY

Allergic airway recall responses require IL-9 from resident memory CD4⁺ T cells

Benjamin J. Ulrich^{1†}, **Rakshin Kharwadkar**^{2†}, **Michelle Chu**¹, **Abigail Pajulas**¹,
Charanya Muralidharan², **Byunghee Koh**^{1,3}, **Yongyao Fu**¹, **Hongyu Gao**⁴, **Tristan A. Hayes**^{1,3},
Hong-Ming Zhou^{5,6}, **Nick P. Goplen**⁷, **Andrew S. Nelson**^{1,3}, **Yunlong Liu**⁴, **Amelia K. Linnemann**^{2,3},
Matthew J. Turner^{5,6}, **Paula Licona-Limón**⁸, **Richard A. Flavell**^{9,10}, **Jie Sun**⁷, **Mark H. Kaplan**^{1,3*}

Asthma is a chronic inflammatory lung disease with intermittent flares predominately mediated through memory T cells. Yet, the identity of long-term memory cells that mediate allergic recall responses is not well defined. In this report, using a mouse model of chronic allergen exposure followed by an allergen-free rest period, we characterized a subpopulation of CD4⁺ T cells that secreted IL-9 as an obligate effector cytokine. IL-9–secreting cells had a resident memory T cell phenotype, and blocking IL-9 during a recall challenge or deleting IL-9 from T cells significantly diminished airway inflammation and airway hyperreactivity. T cells secreted IL-9 in an allergen recall–specific manner, and secretion was amplified by IL-33. Using scRNA-seq and scATAC-seq, we defined the cellular identity of a distinct population of T cells with a proallergic cytokine pattern. Thus, in a recall model of allergic airway inflammation, IL-9 secretion from a multicytokine-producing CD4⁺ T cell population was required for an allergen recall response.

Copyright © 2022
The Authors, some
rights reserved;
exclusive licensee
American Association
for the Advancement
of Science. No claim
to original U.S.
Government Works

INTRODUCTION

Asthma is a chronic inflammatory lung disease. The majority of atopic asthmatics begin having symptoms as children after exposure to common aeroallergens (1, 2). During the sensitization phase, allergens such as pollen, animal dander, and fungal spores cause infiltration of allergen-specific CD4⁺ T helper 2 (T_H2) cells and subsequent type 2 cell-mediated inflammation (3). Type 2 cytokines including interleukin-4 (IL-4), IL-5, IL-13, and IL-9 promote cellular recruitment of effector cells, including eosinophils (4–7), induction of mucus production (8), and increased airway hyperresponsiveness (9).

Traditional type 2 cytokines, which include IL-4, IL-5, and IL-13, are commonly described in asthma pathogenesis and are targets in various stages of therapeutic clinical trials or practice (10). The specific role of IL-9 is less understood but clearly necessary and sufficient in models of allergic inflammation (11). In atopic children, there is a correlation between IL-9 production from peripheral blood mononuclear cells and IL-9–secreting T cells with serum total immunoglobulin E (IgE) (12–14). In adults allergic to house dust mite (HDM), there is an increase in IL-9 production and the number of IL-9–secreting T_H cells providing a marker for asthma and airway hyperresponsiveness correlating to IgE and asthma severity

(13, 15, 16). Mechanistically in allergic disease models, IL-9 promotes all the major features of airway inflammation associated with asthma (17–20). Blockade of IL-9 through antibodies or genetic deficiency of IL-9 prevents mast cell recruitment and activation, eosinophil infiltration, and pulmonary goblet cell hyperplasia (21, 22). Further defining the function and context of IL-9–secreting T cells in vivo will have implications for human health and disease.

There is significant heterogeneity among and within T_H subsets. A memory T_H2 cell population is particularly pathogenic and expresses high levels of multiple cytokines including IL-5, IL-13, and IL-4 (23). IL-9 may also be produced from pathogenic T_H2 cells, and differentiation from a conventional T_H2 to a pathogenic T_H2 phenotype occurs through chronic antigen stimulation (24–27). IL-9 is also expressed in CD4⁺ T cells after chronic stimulation in the lung and skin and is coproduced with other T_H2 cytokines (15, 28, 29). Thus, IL-9 secretion is a feature of a chronically stimulated proallergic T cell population.

Tissue-resident memory T (Trm) cells are the majority of extra-lymphoid memory T cells (30), and the fraction of Trm cells in human tissues is greater than what is found in mice (31). Yet, the role CD4⁺ Trm cells play in allergic disease is still largely unclear. HDM allergen-specific Trm cells develop during chronic challenge (32), and a study using a chronic HDM model finds that CD4⁺ Trm cells are more stable in the lung than CD8⁺ Trm cells (33, 34). The phenotype and function of tissue-resident cells in the allergic lung environment has not been extensively described. In this report, we defined a distinct population of type 2 cells that secrete IL-9, which was required for the inflammatory recall response in a model of seasonal asthma.

RESULTS

IL-9–secreting CD4⁺ Trm cells are maintained in the lung after chronic allergen challenge

To characterize IL-9–secreting T cells in allergic inflammation, naïve C57BL/6 mice were treated intranasally with *Aspergillus fumigatus* (*A.f.*) extract three times weekly for 6 weeks using a protocol modified

¹Department of Microbiology and Immunology, Indiana University School of Medicine, Indianapolis, IN 46202, USA. ²Department of Biochemistry and Molecular Biology, Indiana University School of Medicine, Indianapolis, IN 46202, USA. ³Department of Pediatrics and Herman B Wells Center for Pediatric Research, Indiana University School of Medicine, Indianapolis, IN 46202, USA. ⁴Department of Medical and Molecular Genetics, Indiana University School of Medicine, Indianapolis, IN 46202, USA.

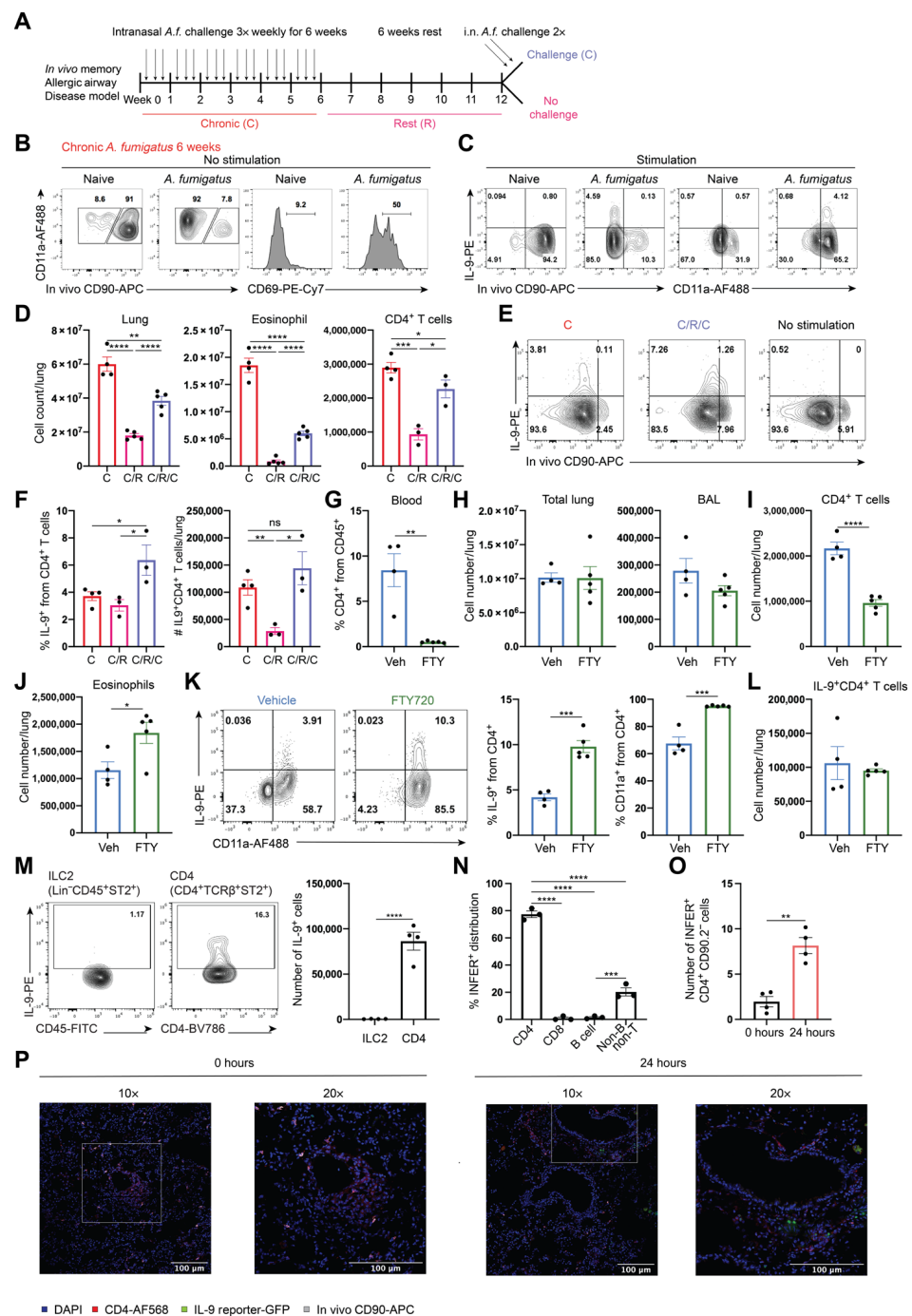
⁵Department of Dermatology, Indiana University School of Medicine, Indianapolis, IN 46202, USA. ⁶Richard L. Roudebush VA Medical Center, Indianapolis, IN 46202, USA.

⁷Thoracic Diseases Research Unit, Division of Pulmonary and Critical Care Medicine, Department of Medicine, Department of Immunology, Mayo Clinic College of Medicine and Science, Rochester, Rochester, MN 55902, USA. ⁸Departamento de Biología Celular y del Desarrollo, Instituto de Fisiología Celular, Universidad Nacional Autónoma de México, Mexico City 04020, Mexico. ⁹Department of Immunobiology, Yale University School of Medicine, New Haven, CT 06510, USA. ¹⁰Howard Hughes Medical Institute, Yale University, New Haven, CT 06510, USA.

*Corresponding author. Email: mkaplan2@iu.edu

†These authors contributed equally to this work.

Fig. 1. IL-9-producing CD4⁺ T cells in a memory allergen recall response. (A) Schematic of the recall allergen chronic/rest/challenge (C/R/C) model. Mice were sensitized intranasally (i.n.) to A.f. three times per week for 6 weeks to develop a chronic response. To generate a memory response, mice were rested for either 6 or 12 weeks without additional manipulation. Recall responses were induced with two doses of A.f. 24 and 48 hours before analysis. (B and C) Flow analysis of isolated lung CD4⁺ T cells without stimulation (B) and with PMA-Ionomycin stimulation (C). (D) Total lung cell number by hemocytometer and eosinophil and CD4⁺ T cell numbers per lung determined using flow cytometry ($n = 4$ to 5). Representative flow plots can be found in fig. S2. (E and F) Flow analysis of IL-9 protein from isolated and stimulated lung CD4⁺ T cells ($n = 3$ to 4). (G to L) Mice were treated with FTY720 for 21 days before recall challenge ($n = 4$ to 5). (G) Flow analysis of peripheral blood CD4⁺ T cells 2 days before the recall challenge. (H) Total Lung and BAL cell number by hemocytometer, (I) CD4⁺ T cell number by flow cytometry, and (J) eosinophil cell number by flow cytometry. (K) Flow analysis of isolated stimulated lung CD4⁺ T cells. (L) IL-9⁺ CD4⁺ T cell numbers per lung. (M) Flow analysis of stimulated lung ILC2 and CD4⁺ T cells ($n = 4$). (N) Distribution of lung IL-9-reporter INFER⁺ cells after C/R/C ($n = 3$). (O and P) Quantification of INFER⁺CD4⁺ CD90.2⁻ cells by immunofluorescence of intact lungs from the recall allergen model. Data are presented as means \pm SEM and are representative of two to three independent experiments. Student's unpaired two-tailed t test was used for comparison to generate P values in (B), (F), (G), (H), (J), (K), (I), (L), (M), and (O). One-way ANOVA with a post hoc Tukey test was used to generate P values in (N). * $P < 0.05$, ** $P < 0.01$, *** $P < 0.001$, **** $P < 0.0001$. ns, not significant.



from a published approach (35) (Fig. 1A and fig. S1A). The chronic allergen exposure resulted in a robust inflammation that was characterized by a large increase of cells in the lung tissue, an influx of eosinophils and CD4⁺ T cells and increased type 2 cytokine production (figs. S1, B and C, and S2, A and B, gating strategy). CD11a and CD69 surface expression and the inability to be labeled by in vivo intravenous CD90 antibody labeling are characteristic of CD4⁺ tissue residency (36, 37). The CD11a⁺ CD69⁺ intravenous CD90⁻ CD4⁺ population was increased upon chronic challenge when compared with either naïve mice (Fig. 1B) or mice challenged with phosphate-buffered saline (PBS) (fig. S1D). To be able to detect intracellular IL-9, CD4⁺ T cells were isolated from the lung and stimulated ex vivo with phorbol 12-myristate 13-acetate (PMA)-Ionomycin with monensin. We observed a distinct IL-9-producing CD4⁺ T cell population after 6 weeks of chronic challenge (Fig. 1C and fig. S1E). All of the IL-9-producing CD4⁺ T cells had a CD11a⁺ intravenous CD90⁻ Trm-like phenotype (Fig. 1C and fig. S1E).

CD4⁺ Trm cells provide a stable pool of cells to mediate asthmatic symptoms in an allergen recall response (34). We wanted to examine whether the IL-9-secreting T cells found in our chronic model (termed “C” in figures) were also found in an allergen recall response that would require memory cells. We “rested” chronically challenged mice from allergen exposure for a minimum of 6 weeks (termed “C/R” in figures) and used a recall challenge to mimic seasonal allergen exposure (termed “C/R/C” in figures) through intranasal rechallenge once daily for 2 days before assessing inflammation (Fig. 1A). We observed a rapid induction of inflammation measured in lung cellularity and eosinophil numbers over 48 hours, albeit to

a lower level than observed after chronic inflammation (Fig. 1D) but significantly greater than when naïve mice were acutely challenged (fig. S1F). In the recall response, the IL-9–secreting population increased in frequency compared with the chronic time point with the majority of the IL-9⁺ cells protected from in vivo antibody labeling (Fig. 1, E and F). There were no IL-9–secreting cells when naïve mice were challenged acutely with allergen (fig. S1, G and H). Although the number of CD4⁺ T cells in the lung waned over time in the absence of allergen, the rapid increase in cell number after challenge approached levels after chronic exposure (Fig. 1F).

To determine whether the IL-9–secreting cells were maintained long term, we performed a longitudinal resting time course. Even after more than 6 months of rest, the CD4⁺ Trm cell pool maintained the ability to produce IL-9 (fig. S3A). Whereas there was a gradual decrease in total IL-9–secreting T cell number (fig. S3A), it was relatively modest and similar to what is observed in the Trm pool (32). Together, these data suggest that IL-9–secreting Trm cells are maintained and respond to allergen reexposure.

To determine whether IL-9–secreting T cells maintain their presence in the tissue over time, we used FTY720, an inhibitor of lymphocyte egress from secondary lymphoid organs. Continuous treatment with FTY720 over several weeks depletes circulating lymphocytes and results in an accumulation of cells in lymphoid organs (38–40). However, treatment with FTY720 should not affect resident cells in tissues such as the lungs, and the IL-9–secreting T cell population should remain intact if they are Trm cells. Mice in the recall model were treated daily with vehicle or FTY720 for the last 3 weeks of the resting phase before allergen rechallenge. Blood drawn at the end of the FTY720 administration contained very few CD4⁺ T cells after FTY720 administration, confirming the loss of circulating T lymphocytes (Fig. 1G). Total cellularity between the FTY720-treated and control groups was similar in the lung and bronchoalveolar lavage (BAL) (Fig. 1H). Because circulating effector T cells are retained in the lymph node with FTY720 treatment, we observed a decrease in the number of CD4⁺ T cells with a concomitant increase in the proportion of eosinophils in the lung (Fig. 1, I and J). The frequency of IL-9–secreting cells was significantly increased in the mice that received FTY720, and there were similar numbers of IL-9–secreting cells in both groups of mice (Fig. 1, K and L). Moreover, almost all the cells in the FTY720-treated mice were CD11a⁺ (Fig. 1K). These data added support for the presence of a resident IL-9–secreting CD4⁺ population that is maintained in the lung in the absence of continued allergen exposure.

In the context of the recall response, we wanted to determine whether IL-9 was produced by populations other than resident T cells. Among IL-9–producing cells, the most abundant producers are T cells and type 2 innate lymphoid cells (ILC2s) (41, 42). Comparing intracellular IL-9 secretion from both CD4⁺ T cells and ILC2s at the recall time point, a much higher total number of CD4⁺ T cells produced IL-9 than ILC2s (Fig. 1M and fig. S2C, gating strategy). To detect IL-9–expressing cells *in situ*, the interleukin nine fluorescent reporter (INFER) IL-9 reporter mouse that allows for IL-9 and green fluorescent protein (GFP) expression through an internal ribosomal entry site–GFP knock-in allele was used (18, 43). By gating on all the INFER⁺ cells from the whole lung, we determined that the majority were CD4⁺ (Fig. 1N). Thus, CD4⁺ T cells are the predominant contributor of IL-9–producing cells in a recall model of allergen exposure.

To further define the localization of the IL-9–secreting T cell population, we performed immunofluorescence on tissue sections

from INFER mice before and after recall challenge. Although there were no detectable GFP⁺ cells before allergen challenge, 24 hours after challenge, CD4⁺ GFP⁺ cells were observed in tissue adjacent to airways in the lung (Fig. 1, O and P). These cells did not stain with the in vivo CD90 antibody, confirming the flow cytometric analysis that these are separable populations (Fig. 1P). Overall, these results define a population of IL-9–secreting tissue-resident CD4⁺ T cells in the lungs after chronic allergen exposure.

Rapid and transient IL-9 production from a resident T cell population

To further define the function of IL-9–secreting T cells, we determined the kinetics of IL-9 production at increasing time points during the recall response (Fig. 2A). Although there was little change in the total cell number in the lung in the first 24 hours, there was a twofold increase in lung cellularity 48 hours after challenge (Fig. 2B). At early time points in a recall response, neutrophils made up a large portion of the initial cellularity before increases in eosinophils and macrophages (Fig. 2C). Upon stimulation *ex vivo* with PMA/ionomycin, CD4⁺ T cells expressed increasing levels of both IL-9 protein and IL-9 reporter (18) over time (Fig. 2D). In unstimulated CD4⁺ T cells taken directly from the lung, IL-9 reporter–positive cell frequency increased over time (Fig. 2E). When examined in the context of intravenous antibody labeling, all the IL-9–producing cells identified by the INFER reporter were in the resident population protected from antibody labeling (Fig. 2E). When IL-9 production was measured from isolated lung CD4⁺ T cells through a 72-hour *ex vivo* culture with antigen-presenting cells and *A. fumigatus*, T cells isolated from early time points of the recall response were primed to secrete IL-9 (Fig. 2F). The activation and expansion of the IL-9–expressing population were evident from the increased cell size of the INFER⁺ but not INFER⁻ CD4⁺ cells and that the ST2⁺ population (which encompass the IL-9–secreting population; Fig. 1M), but not the ST2⁻ population, was positive for Ki67 after allergen challenge (fig. S3, B and C).

We then examined kinetics of *Iil9* transcription in CD4⁺ T cells directly isolated from the lung throughout the recall time course. *Iil9* was rapidly induced by 8 hours after challenge but fell markedly at later time points (Fig. 2G). These data along with the higher early IL-9 secretion in the *ex vivo* coculture model support the concept that IL-9 is transcribed and secreted early in the recall response. *Iil9* transcription was similar to the pattern of expression of *Iil5* but contrasted with *Iil4* and *Iil13* that were induced early but had sustained expression over the period of the challenges and *Iil10* that increased throughout the challenge period (Fig. 2, G and H). Although many of the transcription factors that are required for *Iil9* expression were induced (11, 44), *Spi1* and *Pparg* showed transient induction, similar to *Iil9* itself (Fig. 2I).

CD4⁺ T cell IL-9 production is antigen specific and amplified by IL-33

To demonstrate that IL-9–producing T cells were activated during challenge, we examined the induction of CD69 expression on IL-9⁻GFP⁺ T cells. Eight hours after challenge, IL-9 reporter–positive cells had increased CD69 expression (Fig. 3A). Early activation indicated that cytokine responsiveness to the innate cytokines IL-25, thymic stromal lymphopoietin, and IL-33 that have been linked to T cell responses might be altered (45). We measured the expression of the innate cytokine receptors on CD4⁺ T cells isolated at the

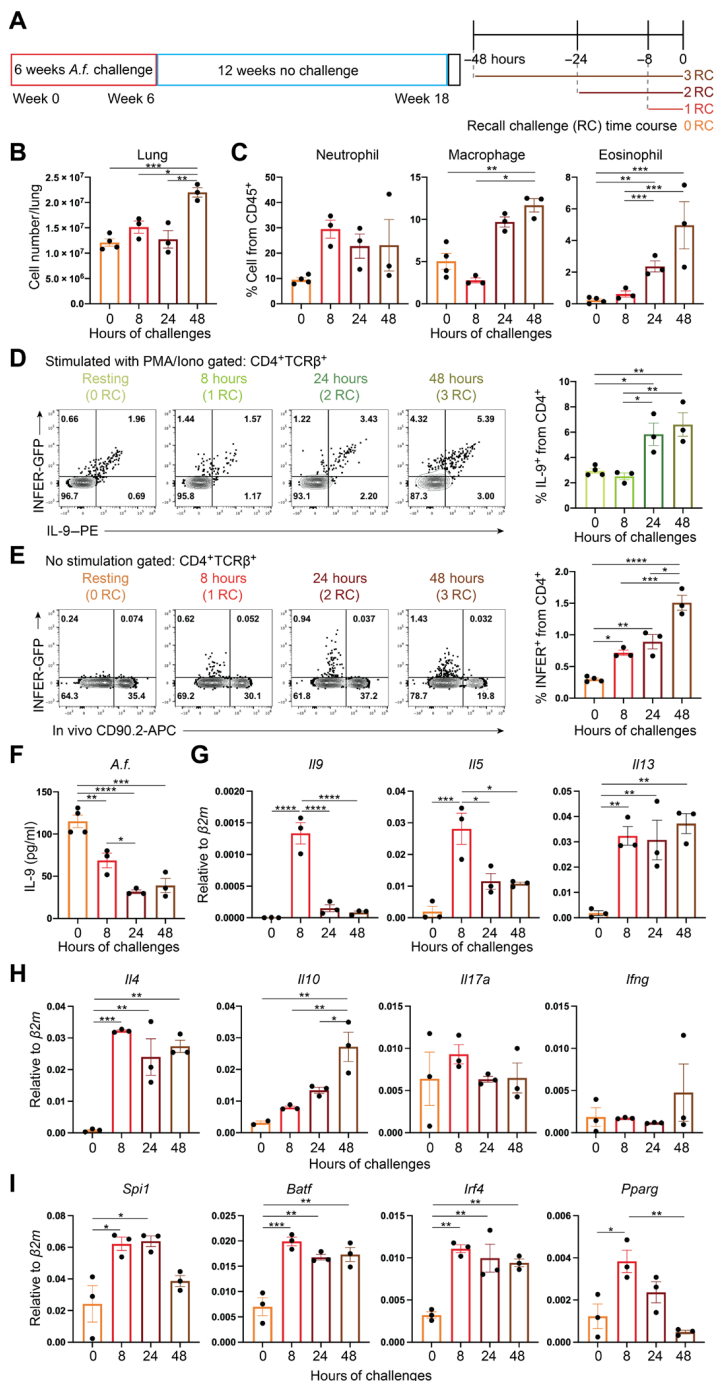


Fig. 2. IL-9 is a memory cytokine in a recall challenge time course. (A) Schematic of the recall allergen time course model. Cells from the chronic/rest/challenge (C/R/C) model described in Fig. 1A were taken for analysis at the indicated time points. (B) Total lung cell numbers by hemocytometer throughout the time course ($n = 3$ to 4). (C) Lung granulocyte frequency by flow cytometry from hematopoietic CD45⁺ cells ($n = 3$ to 4). (D and E) Flow analysis of isolated lung CD4⁺ T cells (D) stimulated with PMA/ionomycin or (E) unstimulated ($n = 3$ to 4). (F) IL-9 protein from ex vivo cytokine assay. Purified CD4⁺ T cells from the recall model were cocultured with an equal number of CD11c⁺ antigen-presenting cells purified from naïve mice and *A.f.* extract for 72 hours. Supernatants were analyzed for IL-9 by ELISA. ($n = 3$ to 4). (G to I) mRNA expression of (G and H) cytokine and (I) transcription factors in unstimulated CD4⁺ T cells isolated from lung ($n = 3$). Data are presented as means \pm SEM and are representative of two independent experiments. One-way ANOVA with a post hoc Tukey test was used to generate *P* values for all comparisons. **P* < 0.05, ***P* < 0.01, ****P* < 0.001, *****P* < 0.0001.

end of the chronic and recall challenge and found *Il1rl1*, the gene encoding for the IL-33 receptor ST2, to be highly expressed (Fig. 3B). *Il1rl1* was highly expressed in T cells after chronic challenge and further induced after a recall challenge, with greater than 90% of IL-9-secreting cells expressing the ST2 receptor (Fig. 3, B and C). *Il1rl1* expression was enriched in the CD4⁺ IL-9 reporter-positive cells (Fig. 3D). The induction of IL-33 in the BAL fluid mirrored the transient expression of IL-9 (Fig. 3E). All of the innate cytokines had some ability to amplify IL-9, although IL-33 was clearly the most potent (Fig. 3F).

We then wanted to distinguish between antigen-stimulated and cytokine-stimulated IL-9 production after allergen recall challenge. We compared recall challenge with *A. fumigatus* and IL-33. Recall challenge with *A. fumigatus* resulted in greater cellular recruitment to the lung and expansion of CD4⁺ T cells than IL-33 (Fig. 3, G and H). IL-33 failed to induce significant IL-9 production when administered alone in vivo and did not prime T cells for IL-9 production when cells were stimulated with *A. fumigatus* during culture ex vivo (Fig. 3, I and J). We then defined the contribution of IL-33 using *Il1rl1*^{-/-} mice that are deficient for the IL-33 receptor ST2. Deficiency of ST2 resulted in reduced accumulation of CD4⁺ T cells, ILC2, and regulatory T cells (T_{regs}) after recall challenge, compared with control mice (Fig. 3, K and L). ST2-deficient mice also displayed a significant decrease in the production of type 2 cytokines, including IL-9, IL-13, and IL-5 by CD4⁺ T cells in the lung, compared with control mice (Fig. 3, M and N). ST2-deficient CD4⁺ T cells stimulated ex vivo with *A. fumigatus*, and IL-33 showed diminished IL-9 production compared with wild-type controls (Fig. 3O). Allergen was capable of stimulating IL-9 production from lung CD4⁺ T cells at all stages of the model, and this response was allergen specific, because use of bovine serum albumin (BSA), *Alternaria alternata* (*A.a.*), or HDM extract as stimuli did not elicit IL-9 production (Fig. 3, P and Q).

To confirm the requirement for allergen in the recall response, we treated mice with anti-major histocompatibility complex II (MHC-II) antibody during the recall challenge (46). Blockade of MHC-II led to a decrease in total number of cells in both lung and lymph nodes compared with the mice that received isotype control antibody (Fig. 3R). In addition, MHC-II blockade resulted in a significant decrease in the total number of CD4⁺ T cells and IL-9-producing CD4⁺ T cell populations in the lung after the recall response (Fig. 3, S to U). Together, these data suggest that production of IL-9 in a resident memory population is dependent on allergen recall and amplified by IL-33.

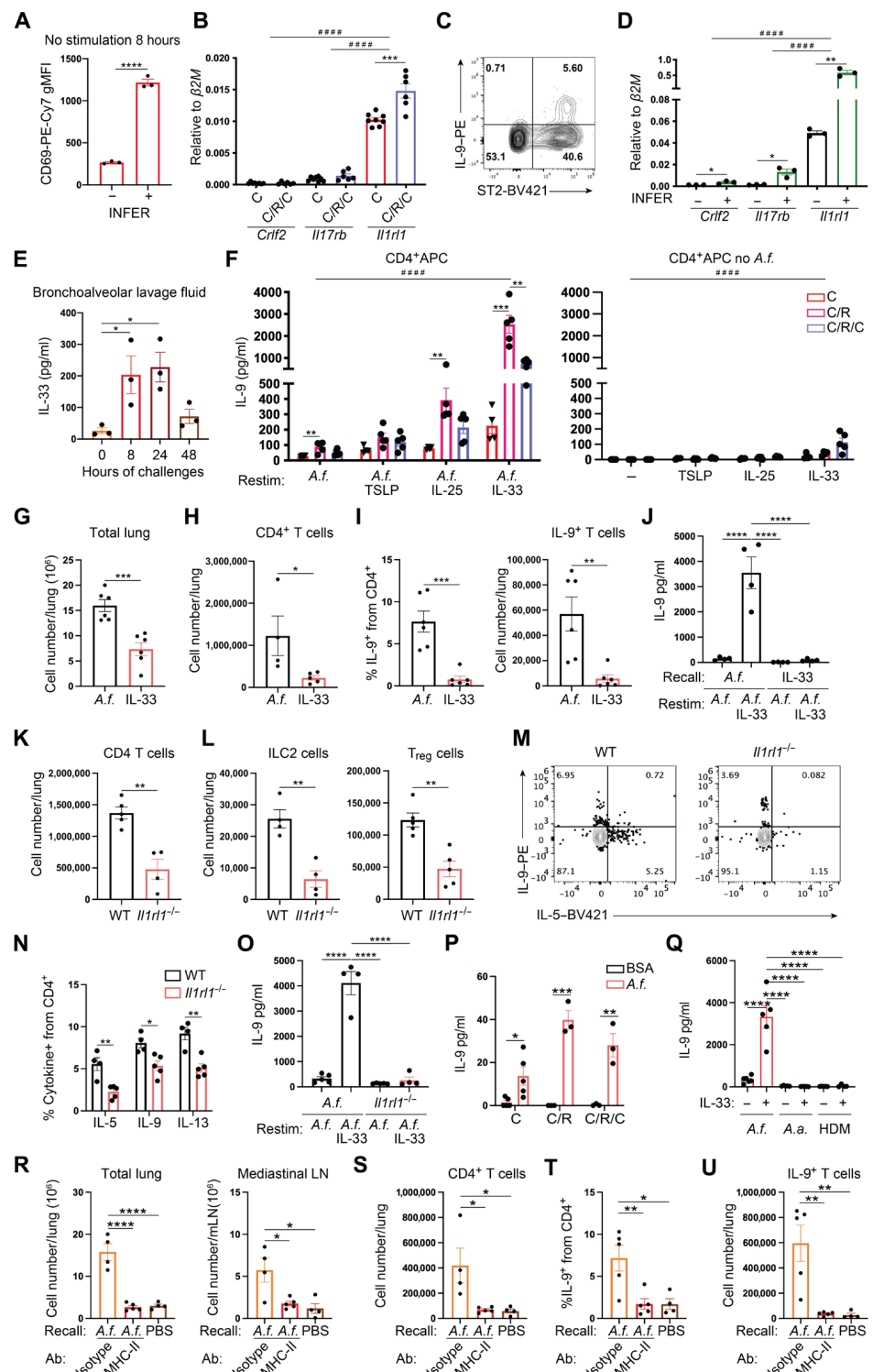
High IL-9 expression distinguishes a multicytokin e-secreting phenotype

In defining the identity of the IL-9-secreting T cell population, a critical question was whether these cells had a polarized phenotype, expressing IL-9 alone, or whether IL-9-producing cells also expressed other cytokines. Flow cytometric analysis of cells stimulated ex vivo revealed extensive overlap in IL-9 production with IL-5, IL-10, and IL-13, and IL-9 was expressed in the majority of T cells with a (Fig. 4, A and B). However, IL-9 production was distinct from those producing IL-4 and IL-2 (Fig. 4A and fig. S4A).

To further characterize these populations, we enriched for IL-9-secreting cells from the lungs of mice in the recall model by sorting for CD4⁺ ST2⁺ cells after one recall challenge 8 hours before (maximal *Ii9* transcription in Fig. 2F) and compared them with sorted CD4⁺ ST2⁻ cells through single-cell RNA sequencing (scRNA-seq).

Fig. 3. IL-9 secretion is antigen specific and enhanced in the presence of IL-33. (A) Flow analysis of isolated lung CD4⁺ T cells 8 hours after recall challenge ($n=3$). (B) mRNA expression in unstimulated lung CD4⁺ T cells ($n=6$ to 8). (C) Flow staining of isolated lung CD4⁺ T cells stimulated with PMA/ionomycin. (D) mRNA expression in flow-sorted lung CD4⁺ T cells at the chronic time point ($n=3$). (E) IL-33 protein levels in the BAL fluid determined using ELISA ($n=3$). (F) IL-9 protein from T cells stimulated ex vivo with A.f. (left) or without A.f. (right) ($n=4$). (G to J) Mice were treated with either A.f. or IL-33 during the recall challenge ($n=4$ to 5). (G) Total lung cell number by hemocytometer and (H) CD4⁺ cell numbers using flow cytometry. (I) Frequency and number per lung of IL-9⁺ from CD4⁺ using flow cytometry. (J) IL-9 protein from T cells stimulated ex vivo with allergen extract. (K to O) The recall allergen model was used to compare wild-type (WT) and *Il1rl1*-deficient mice ($n=4$ to 5). (K) Lung CD4⁺ T cell, (L) ILC2 cell, and T_{reg} numbers by flow cytometry. (M and N) Flow analysis of isolated CD4⁺ lung cells stimulated with PMA/ionomycin. Representative dot plot (M) and averages of multiple mice (N) are shown. (O) IL-9 protein from ex vivo cytokine assay. (P) IL-9 protein from ex vivo T cell stimulation with either BSA or A.f. ($n=3$ to 4). (Q) IL-9 protein from ex vivo T cell stimulation with A.f., A.a., or HDM allergen ($n=3$ to 4). (R to U), Mice were either treated intravenously with anti-MHC-II or isotype control antibody before and during the recall response or examined without recall challenge (PBS treated) ($n=4$ to 5). (R) Total lung cell, mediastinal lymph node, and (S) lung CD4⁺ T cell number. (T) Flow analysis of isolated lung CD4⁺ T cells stimulated with PMA/ionomycin. (U) IL-9⁺ CD4⁺ T cell number. Data are presented as means \pm SEM and are representative of two experiments. Student's unpaired two-tailed *t* test was used for comparison to generate *P* values in (A), (B), and (D) (INFER +/− comparison), (E), (G to L), (N), and (P). One-way ANOVA with a post hoc Tukey test was used to generate *P* values in (F) (groups with same innate treatment), (J), (O), and (Q) to (U). Two-way ANOVA with a post hoc Tukey test was used to generate *P* values in (D) and (F). **P* < 0.05, ***P* < 0.01, ****P* < 0.001, *****P* < 0.0001, and #####*P* < 0.00001. In (B), (D), and (F), * indicates a comparison between time points or conditions, and # designates a comparison between innate cytokine or receptors. Ab, antibody; gMFI, geometric mean fluorescence intensity.

The predominant ST2[−] populations had a naïve phenotype (high *Sell* and *Ccr7*, low *Cd44*) with a small population of ST2[−] T_{regs} (Fig. 4, C and D, and fig. S4B). The ST2⁺ cells were more heterogeneous with CD4⁺ populations of macrophage and myeloid cells, natural killer T (NKT) cells, T_{regs}, type 2 T cells, and nonpolarized but activated cells (Fig. 4, C and D; fig. S4C; and data file S1). The *Il9*-expressing population overlapped with *Il5*- and *Il13*-expressing cells (Fig. 4D). Excluding the myeloid, NKT, and T_{reg} populations, we performed pseudotime analysis and observed predicted development from naïve cells to nonpolarized activated cells, to the most differentiated cells that expressed multiple type 2 cytokines (Fig. 4, E and F). In addition, transcription factors



associated with T_H9 cell differentiation such as *Irf4*, *Irf8*, and *Stat5a* were highest in the most differentiated cells (fig. S4D).

We then defined subsets of these cells based on cytokine secretion patterns in the transcriptome as defined in the “scRNA-seq and analysis” section; cells expressing IL-9 without T_H2 cytokine (*Il13* and *Il5*) expression were termed T_H9, cells expressing T_H2 cytokines and no *Il9* were termed T_H2, and cells coexpressing *Il9* and T_H2 cytokines

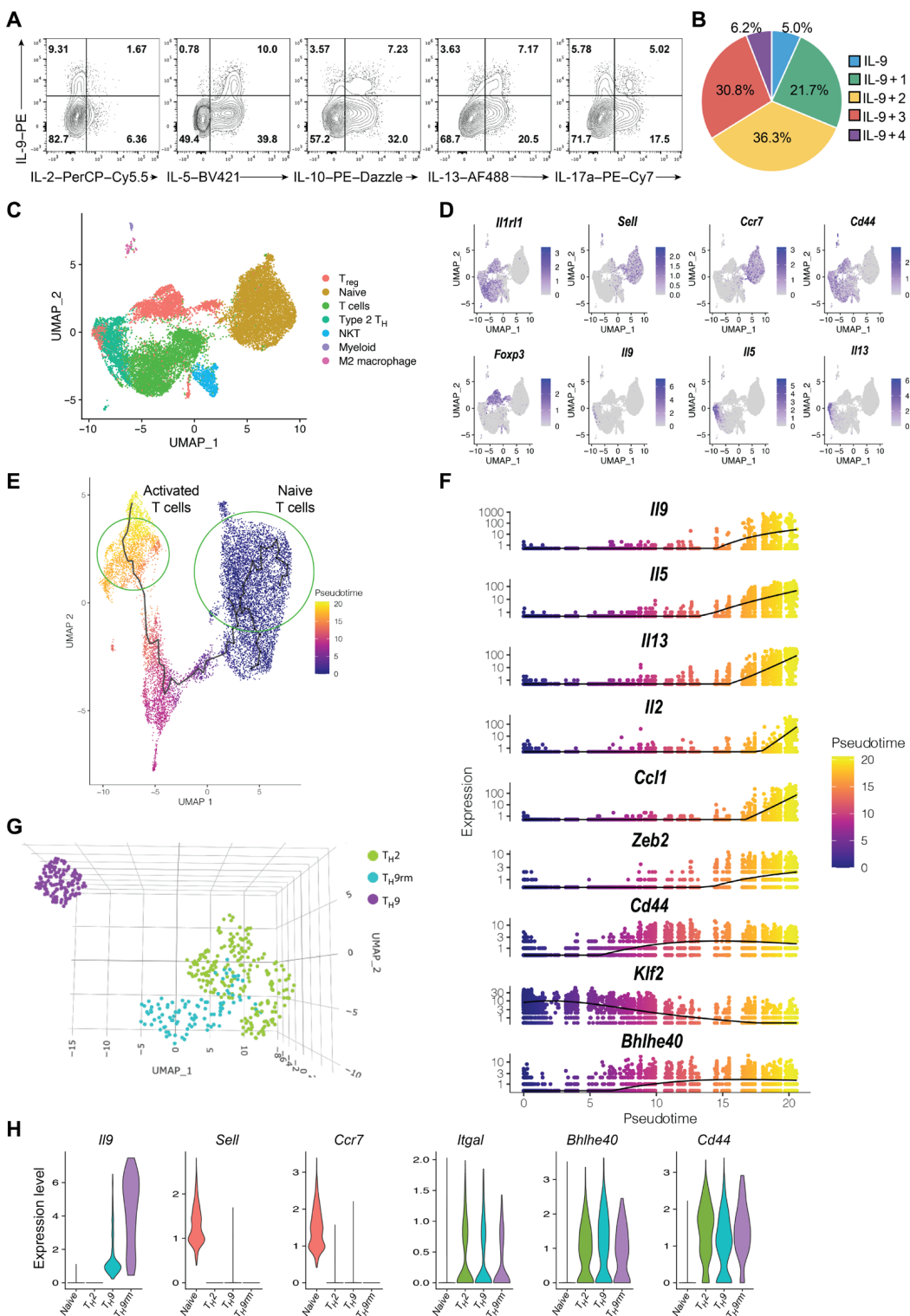


Fig. 4. IL-9-secreting CD4⁺ Trm cells represent a unique differentiated population. (A and B) Flow cytometry analysis of isolated lung CD4⁺ T cells after recall allergen and stimulated with PMA/ionomycin in vitro. (B) Percentages of multicytokine-positive cells in the IL-9⁺ population. (C to H) scRNA-seq analysis of lung CD4⁺ T cells from *A.f.* recall allergen-challenged mice; five mice were pooled per group before fluorescence-activated cell sorting (FACS) of CD4⁺ ST2⁺ and CD4⁺ST2⁻ cells (C) Unsupervised UMAP with clustering based on gene expression. (D) Log-fold gene expression over UMAP of the indicated genes. (E) Pseudotime trajectory analysis over naive (right circle) and activated T cell populations (left circle). (F) Plot of log-fold expression of the indicated genes as a function of pseudotime. (G) Plot of unsupervised UMAP clustering of T_H2, T_H9rm, and T_H9 cell populations. (H) Violin plots of log-fold expression of the indicated genes across naïve, T_H2, T_H9, and T_H9rm cell populations.

were defined as a T_H9 resident memory (T_H9rm) population. Uniform Manifold Approximation and Projection (UMAP) analyses indicated that the T_H9 population was separate from the T_H2 and T_H9rm populations (Fig. 4G). Violin plots of gene expression in these subsets indicated shared expression of multiple genes that distinguished them from naïve cells including *Cd44*, *Il2ra*, and *Bhlhe40* (Fig. 4H). *Il9* expression was greater in the T_H9rm population than in the T_H9 population (Fig. 4H). T cell activation–associated genes *Il2ra* and *Bcl2l1* were enriched in T_H2 and T_H9rm populations and showed lower expression of *Klf2* and *Tcf7* compared with naïve and T_H9 cell subsets (fig. S4E). T_H2 and T_H9rm populations had similar levels of genes such as *Il2* and *Ccl1*. *Zeb2* and *Stat5a* were highest in T_H2 and T_H9rm, respectively, demonstrating differential gene expression between these two populations (fig. S4E). A heatmap of the differentially expressed genes among the subsets and pairwise comparisons between the populations using volcano plots further demonstrated separation in cellular identity (fig. S5, A to C, and tables S3 to S5).

Chromatin structure distinguishes T_H2 and T_H9rm populations

The distinctions in the cellular identity of IL-9–secreting T cells were further defined using a single-cell assay for transposase-accessible chromatin using sequencing (scATAC-seq) analysis of nuclei from CD4⁺ ST2⁺ cells after recall challenge. The scATAC-seq data were integrated with the scRNA-seq analysis for CD4⁺ ST2⁺ cells to identify cell phenotypes including T_H2, T_H9, T_H9rm, and T_{regs} (Fig. 5A). Using chromatin structure to subset the population, we could not identify T_H9 cells because there were no cells that had an open *Il9* locus but did not have an open T_H2 cytokine locus. This finding suggested that cells distinguished transcriptionally as T_H9 were related to T_H9rm by chromatin structure. We included analysis of the T_{reg} population for comparison. The chromatin structure of T_H2 cells was quite distinct from T_H9rm cells, which had much more heterogeneous chromatin structure (Fig. 5A). Consistent with all populations being ST2⁺, there was equal accessibility at the *Il1rl1* locus in each subset (Fig. 5B). The T_H2 population demonstrated more accessibility at T_H2 cytokine loci and adjacent regulatory regions including *Il4*, *Il13*, *Il5*, and *Rad50*. T_H9rm cells showed some accessibility at the *Il4*, *Il13*, and *Rad50* locus but not at *Il5* loci (Fig. 5C). At the *Il9* gene locus, there was chromatin accessibility in T_H9rm cells that was not present in T_H2 or T_{regs}, and Foxp3 accessibility was highly enriched in T_{regs} (Fig. 5, D and E). Unsupervised clustering of genes that were more accessible in T_H9rm or T_H2 revealed additional loci that had open chromatin regions (fig. S5D). We then performed an analysis of transcription factor binding sites that were enriched within open chromatin regions in each of the subsets of cells. We observed enrichment of binding sites for a number of characterized factors including BATF/Jun, GATA3, and PPAR γ in T_H2 cells (Fig. 5F), all factors that are associated with primary or tissue-associated T_H2 cytokines (29, 47). The T_H9rm population showed enrichment of binding sites for several distinct factors, including VDR and BHLHE40, but were represented in a smaller proportion of the open regions, parallel to the more diffuse chromatin structure observed in the T_H9rm population (Fig. 5F). We further examined the chromatin structure at the loci of transcription factors and saw that E26 transformation specific (ETS) proteins including *Spi1* and *Fli1* were more active in T_H9rm cells, whereas *Gata3* and *Irf4* were more active in T_H2 cells (Fig. 5G). Together, these data identified a discrete population of proallergic

cytokine-producing cells that have an identity distinct from classically defined T_H2 cells.

IL-9 is required for the allergen recall response

Having established the presence of a multicytokine-producing resident T_H population, we wanted to define the importance of IL-9 in the response to allergen challenge. To test the requirement for IL-9 in the recall response, we used neutralizing antibodies to IL-9 administered before and during the rechallenge phase (Fig. 6A). The anti-IL-9 blockade significantly reduced the inflammatory cellularity in the lungs of mice compared with control numbers (Fig. 6, B and C). To determine whether anti-IL-9 blockade has therapeutic value preventing allergic airway hyperresponsiveness in a recall response, airway resistance was measured. The anti-IL-9 treatment reduced the airway hyperresponsiveness to a level similar to naïve mice and was significantly reduced when compared with isotype control–treated mice (Fig. 6D). To place the effects of anti-IL-9 in the context of an additional type 2 cytokine required in allergic airway inflammation (14), we compared the efficacy of anti-IL-9, anti-IL-13, or isotype control antibodies in attenuating inflammation. Anti-IL-9 blockade reduced lung cellularity more than the anti-IL-13 blockade, whereas BAL numbers were not altered in any of the treatments (Fig. 6E). The anti-IL-9 treatment group had a reduced cell number, as determined by flow cytometry, in most of the granulocyte and lymphocyte populations examined (Fig. 6F). Several populations that were diminished with anti-IL-9 including B cells were unaltered with anti-IL-13 treatment. Other cell populations showed reduced numbers in both the anti-IL-9 and anti-IL-13 treatments (Fig. 6G).

Although these data on a therapeutic benefit of anti-IL-9 treatment are consistent with a number of published reports on the effects of anti-IL-9 in acute models (14, 48), they are different from what has been observed with patients (49, 50). We speculated that mice with chronic allergen exposure might have a different response when compared with the recall model that better represents intermittent or seasonal exposure. To test this, we examined the effects of anti-IL-9 at the chronic 6-week time point. When anti-IL-9 treatment was provided to mice for the last week of the 6-week exposure (Fig. 6H), there was not a difference in cellularity in the lung or the BAL (Fig. 6I). Airway hyperresponsiveness in the chronic model was unchanged between the anti-IL-9 and isotype treatment groups, although airway hyperresponsiveness increased compared with naïve controls (Fig. 6J). Although there was a reduction in B cells with the blockade of IL-9, other populations including CD4⁺ T cells that were diminished in number in the recall model were not altered by treatment at the chronic 6-week time point (Fig. 6, K and L). Thus, in contrast to the recall model, anti-IL-9 therapy administered in the chronic allergen response did not demonstrate a reduced inflammatory infiltrate.

To demonstrate that IL-9 promoting the inflammation was specifically from T cells, we generated an *Il9 fl/fl* mouse (fig. S6, A and B) and crossed it to a CD4-Cre transgenic mouse. T_H9 cells generated from *Il9 fl/fl Cd4-cre*⁺ mice did not generate IL-9 in vitro (fig. S6, C to E). In contrast, *Il9 fl/fl Cd4-cre*⁺ and control mice had ILC2 and NK cells that produced similar amounts of IL-9 and other cytokines after IL-33 challenge (fig. S6, F and I). Peritoneal-derived mast cells from *Il9 fl/fl Cd4-cre*⁺ and control mice also produced similar IL-9 (fig. S6J).

In the recall model, the *Il9 fl/fl Cd4-cre* mouse had a reduction in effector cell numbers including CD4⁺ T cells, CD8⁺ T cells, B cells,

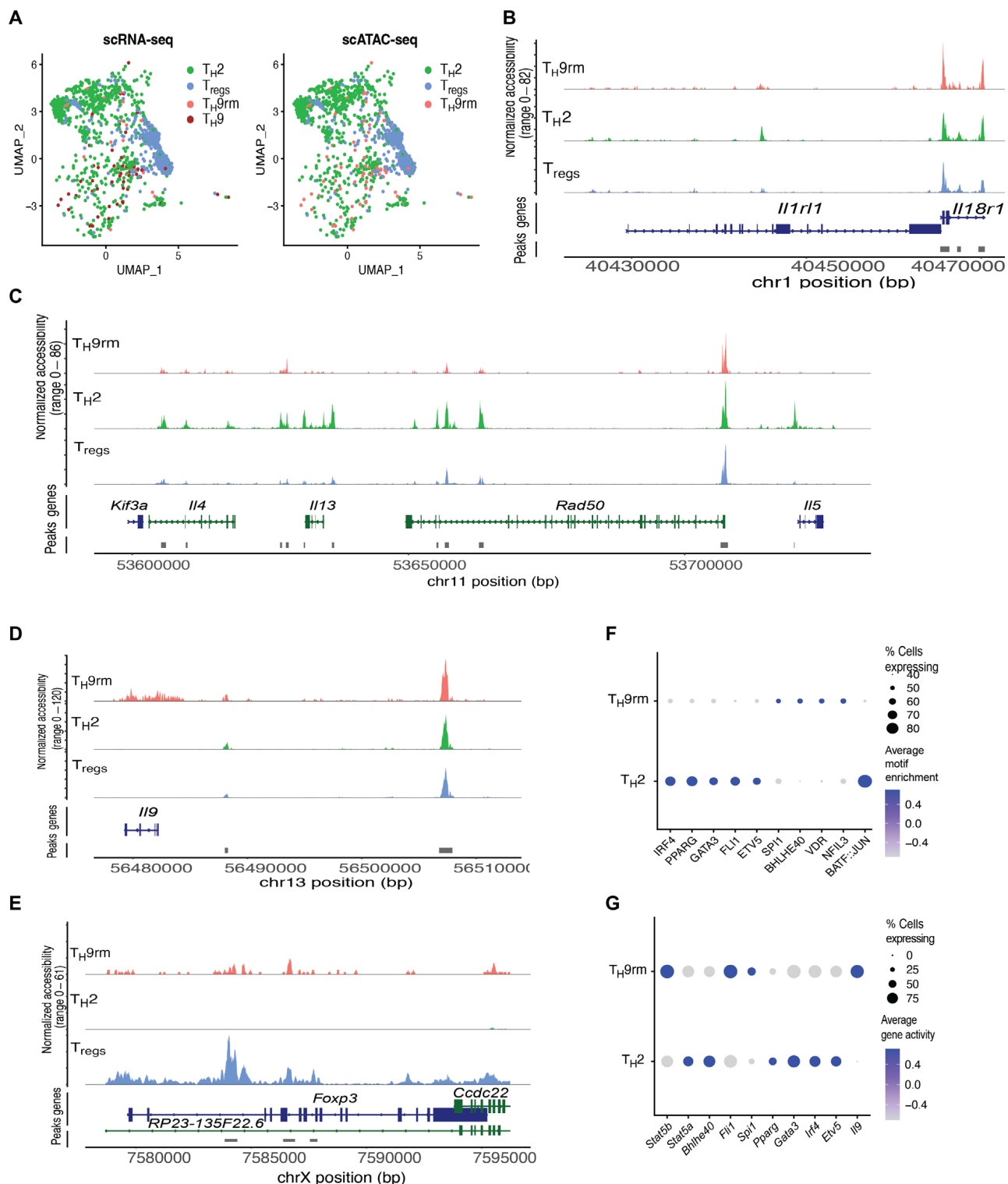


Fig. 5. Chromatin structure distinguishes T_H2 and T_H9rm populations in the memory recall model. scACTC-seq analysis for lung CD4⁺ T cells from *A. f.* recall allergen-challenged mice; five mice were pooled per group before FACS sorting of ST2⁺ CD4⁺. (A) UMAP of ST2⁺ CD4⁺ T cells clusters derived from integrative analysis of scRNA-seq and scATAC-seq, showing T_H9rm, T_H2, and T_{reg} populations. (B to E) ATAC-seq profiles with peaks indicating chromatin accessibility at each locus generated using CoveragePlot function in Seurat. (F) Differentially enriched motifs for transcription factors in T_H9rm and T_H2 populations determined by performing ChromVar analysis. (G) Gene activity determined by using Seurat/Findmarkers based on open promoter regions within 2-kb upstream of the promoter. Results are shown for transcription factors associated with IL-9 expression in T_H9rm and T_H2 cells.

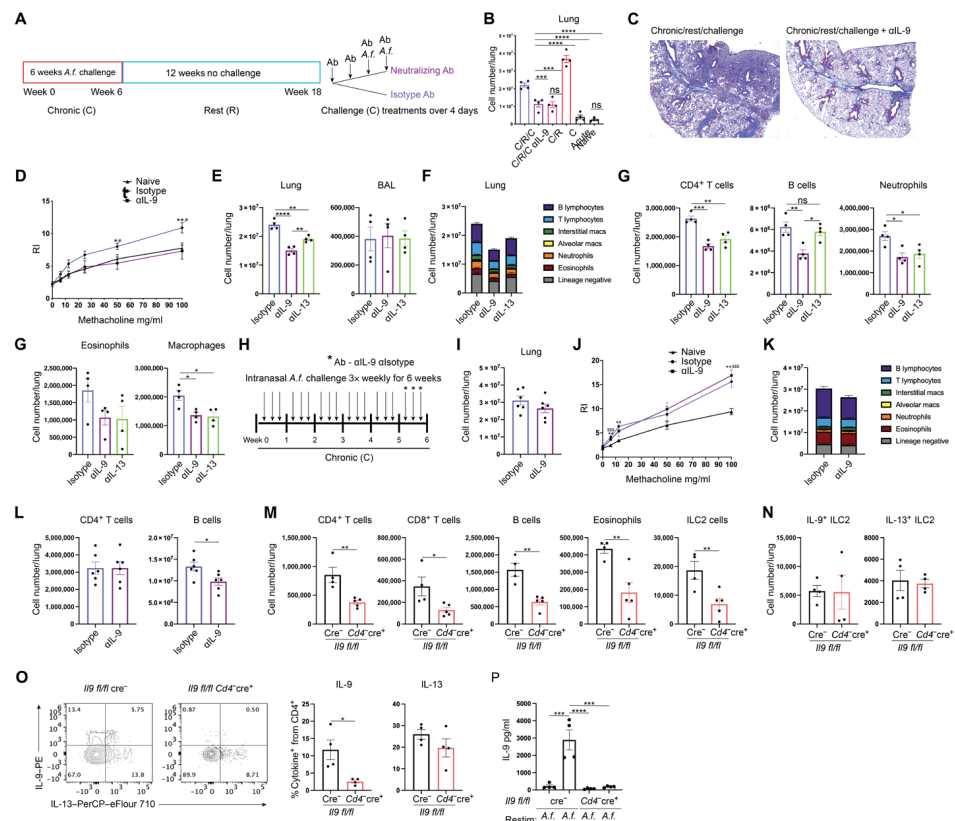


Fig. 6. Anti-IL-9 at the recall challenge phase blocks cell expansion and inflammation. (A to G) Mice were either intranasally treated with IL-9-neutralizing or isotype control antibody before and during the recall allergen response ($n = 5$ to 7). (A) Schematic of the recall antigen antibody blockade model. Similar to the recall allergen chronic/rest/challenge (C/R/C) model described in Fig. 1A, in the recall response, mice were intranasally treated with IL-9-neutralizing or isotype control antibody before and during the recall allergen response. (B) Total lung cell numbers by hemocytometer. (C) Paraffin-embedded lung lobe sections were stained with Masson's trichrome. (D) Airway resistance 24 hours after the last intranasal A.f. treatment was measured after intubation and intratracheal challenge with increasing doses of methacholine. Student's unpaired two-tailed *t* test comparing isotype versus naïve represented by * and anti-IL-9 versus isotype by #. (E) Total lung and BAL cell numbers by hemocytometer. (F) Stacked bar graph of lung cell numbers based on flow cytometry. (G) Cell number of lung cell populations by flow cytometry. (H to L) Mice were either intranasally treated with IL-9-neutralizing or isotype control antibody in the last week of the chronic allergen challenge ($n = 6$ to 7). (H) Schematic of the chronic antibody blockade model. Mice were sensitized intranasally to A.f. three times per week for 6 weeks to develop a chronic response. During the last week, mice were intranasally treated with IL-9-neutralizing or isotype control antibody during allergen challenge. (I) Total lung cell numbers by hemocytometer. (J) Airway resistance 24 hours after the last intranasal A.f. treatment was measured after intubation and intratracheal challenge with increasing doses of methacholine. Student's unpaired two-tailed *t* test comparing isotype versus naïve represented by * and anti-IL-9 versus naïve by §. (K) Stacked bar graph of lung cell numbers based on flow cytometry. (L to N) B cell and CD4⁺ cell number per lung. (M to P) Recall allergen model was used to compare Cre- and Cd4^{cre}⁺ II9^{fl/fl} mice ($n = 4$ to 5). (M) Cell number of lung cell populations by flow cytometry. (N) Flow analysis of lung ILC2 cells stimulated with IL-33. (O) Flow analysis of isolated lung CD4⁺ T cells stimulated with PMA/ionomycin. (P) IL-9 protein from ex vivo cytokine assay stimulated with A.f. in the presence or absence of IL-33. Data are presented as means \pm SEM and are representative of two independent experiments. Student's unpaired two-tailed *t* test was used for comparison to generate *P* values in (D), (I), (J), and (L) to (O). One-way ANOVA with a post hoc Tukey test was used to generate *P* values in (B), (E), (G), and (P). **P* < 0.05, ***P* < 0.01, ****P* < 0.001, *****P* < 0.0001.

eosinophils, and ILC2s (Fig. 6M). The frequency of ILC2 cells secreting IL-9 and IL-13 was similar to controls (Fig. 6N). In contrast, CD4⁺ T cells were deficient in production of IL-9 but had IL-13 production that was comparable with controls (Fig. 6, O and P). These data demonstrate that IL-9 from T cells was critical for the recall response in allergic airway disease.

To further characterize the effects of blocking IL-9 during the recall challenge, we performed scRNA-seq on total lung cells from control and anti-IL-9-treated mice. We identified 20 distinguishable clusters of cells (Fig. 7A; fig. S7, A and B; and data file S5). Similar to the flow cytometric analysis, there were only modest changes in the proportions of populations, with decreases in the proportion of B cells, T cells, and ILC2s, and increases in the proportion of

interstitial macrophages and structural cells (fig. S7, A and B). Despite the minor changes in population distribution, there were significant changes in gene expression among the clusters. We observed *Scgb1a1*, *Mgp*, and *Retnla*, all genes associated with lung inflammation, expressed broadly in cell types and uniformly diminished by treatment with anti-IL-9 (Fig. 7B and fig. S8, A and B). Additional changes in gene expression were restricted by cell type.

In the context of the recall response, *Il9* is expressed predominantly by T cells and ILC2s in a pattern that matches preferential expression of *Il1rl1* and *Il2ra* but not other cytokine receptors (Fig. 7C). Focusing on these populations, we observed decreases in genes associated with cell survival and proliferation in ILC2s and T_{reg}s, but not CD4⁺ T cells, suggesting that IL-9 has differential

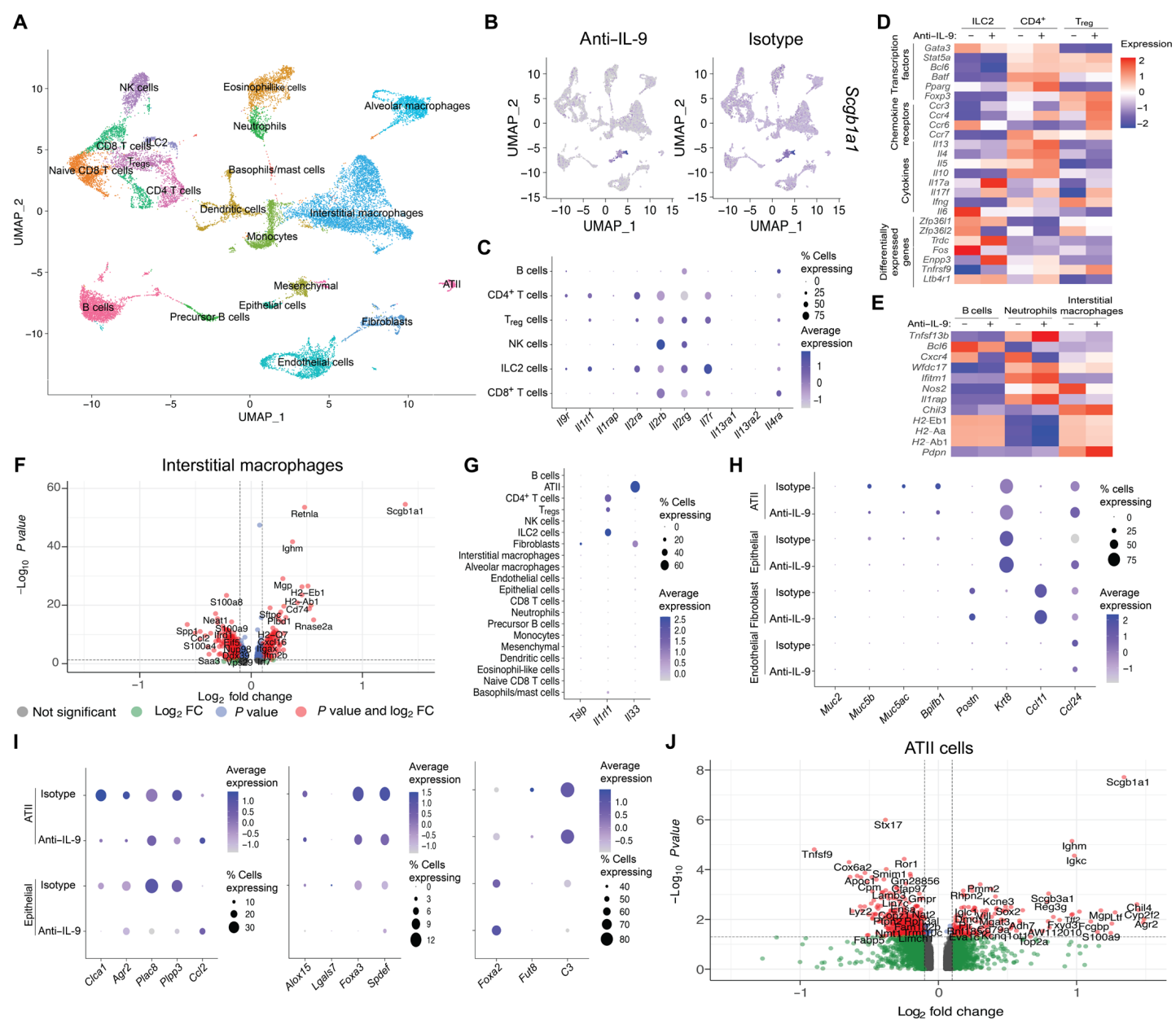


Fig. 7. Blockade of IL-9 in the recall model alters gene expression in multiple lung cell types. (A) UMAP of unsupervised clustering defining cell types in the lung. (B) UMAP feature plot of comparing *Scgb1a1* expression across all cell types with/without anti-IL-9 and isotype treatments. (C) Seurat DotPlot of cytokine receptor expression in lymphoid populations. (D) Heatmap of differentially expressed genes in *Il1rl1* expressing lymphoid populations. (E) Heatmap of differentially expressed genes in B cells, neutrophils, and interstitial macrophages. (F) Volcano plot showing differentially expressed genes based on fold change in interstitial macrophages. FC, fold change. (G) Dot plot of *Il1rl1*, *Il33*, and *Tslp* expression. (H and I) Seurat DotPlot of gene expression patterns in lung structural cells. (J) Volcano plot showing differentially expressed genes based on fold change in ATII cells.

effects on their expansion *in vivo* (fig. S8C). Blockade of IL-9 broadly altered expression of chemokine receptors and cytokines across all cell types (Fig. 7D). Cell type-specific effects included marked decreases in *Klrb1* in CD4⁺ T cells and *Cd69* and *Il6* in ILC2s, coincident with an increase in *Il17a* and, to a lesser degree, *Il17f* in the ILC2 population (Fig. 7D and fig. S8C). Additional changes in gene expression within the ILC2s highlight this population as an IL-9 responder (Fig. 7D). *Zfp36l2*, which is implicated in integrin-mediated cell migration (51–53), was significantly reduced in CD4⁺ T cells, T_{regs}, and ILC2s (Fig. 7D and fig. S8, C to E). IL-9 blockade also had significant effects on gene expression in B cells, neutrophils, and both

alveolar and interstitial macrophages (Fig. 7, E and F, and fig. S8F). In the macrophage populations, blockade of IL-9 reciprocally affected M1 (*Nos2*) and M2 (*Chil3*) markers that would indicate a shift to a less inflammatory phenotype (Fig. 7E). MHC class II antigen presentation genes were also decreased by IL-9 blockade in macrophages (Fig. 7, E and F, and fig. S8F).

Blocking IL-9 also affected gene expression in nonhematopoietic cells, which express low but detectable *Il9r* (fig. S8G). Lung structural cells are primary sources of the innate cytokines that amplify *Il9* production. Production of *Il33* was observed in fibroblasts and type II epithelial cells, whereas *Tslp* was expressed at very low levels

and *Il17e* was undetectable (Fig. 7G). As noted above, *Scgb1a1*, which is expressed in airway epithelial cells during lung inflammation and airway remodeling, was markedly decreased by IL-9 blockade (Fig. 7, B and J) (54, 55). Moreover, the expression of genes associated with lung fibrosis and mucus metaplasia including *Muc2*, *Muc5ac*, *Muc5b*, and *Bpifb1* were significantly reduced in alveolar epithelial type II (ATII) and epithelial cells with anti-IL-9 treatment (Fig. 7H). IL-9 blockade also diminished a set of IL-13-inducible genes in airway epithelial cells, including *Cla1*, *Agr2*, *Alox15*, *Foxa3*, and *Spdef* (Fig. 7I) (54, 56–58), suggesting that IL-9 signaling cooperates with IL-13 in generating this gene expression pattern. The *Alox15* inhibitor *Foxa2* was increased with anti-IL-9 treatment (Fig. 7I) (59). Together, these data demonstrated that a multicytokine-producing T_H cell distinct from classically defined T_H2 and T_H9 cells generated IL-9 that is required for allergic lung inflammation during an allergen recall response.

DISCUSSION

Compared with other T_H subsets, there is very little known about the development and function of IL-9-secreting CD4⁺ T cells within peripheral tissues. It is clear that the cytokine IL-9 is important in allergic airway responses and that chronic stimulation is required to develop IL-9-secreting CD4⁺ T cells (24–27, 35). IL-9 is a cytokine in allergen-specific CD4⁺ T cells that is found in the peripheral blood of allergic and asthmatic patients; this population is diminished after successful immunotherapy (16, 28). We have identified an analogous population in mice that responds rapidly to recall allergen.

The overall kinetics of IL-9 production may be part of the proinflammatory contribution of this Trm population to airway inflammation. IL-9 was produced at high levels within 8 hours after an allergen recall exposure and decreased thereafter. Transient *Il9* expression is seen in culture and other models, peaking over a number of days before dropping to low levels (18, 29, 60). *Il5* also demonstrated early transient expression, although the drop at 24 hours was not as marked. These data suggest that resident memory CD4⁺ T cells may be primed to secrete IL-9 in an immediate response to recall antigen stimulation. However, *Il9* expression was observed in the most differentiated populations of T_H cells in the lung, coexpressed with other classical T_H2 cytokines, suggesting that transient *Il9* production does not represent an intermediate state that transitions to a T_H2 cell. This is similar to observations in a study where *IL9* is expressed in the most differentiated cells among heterogeneous T_H memory populations (61). Pseudotime analysis of scRNA-seq of T_H cells from mice acutely challenged with HDM extract demonstrates a similar end stage with expression of effector cytokines and an intermediate state that had a distinct interferon (IFN)-induced transcriptional signature (62). We did not observe the IFN-induced signature among the CD4⁺ T cells examined here, which was likely due to differences in the models of chronic short-term and allergen recall exposure. Thus, the derivation of the IL-9-secreting resident T cells is still unclear, and whether they arise from or differentiate into classically defined T_H2 cells still needs to be further explored.

Whether IL-9 is involved in patient asthma is still controversial. IL-9-expressing pathogenic T_H2 cells in patients are linked with asthma and HDM sensitization (16). IL-9-expressing T_H2A cells are also suggested to be a highly pathogenic subpopulation (28). Yet, despite numerous reports documenting an effect of blocking

IL-9 in experimental models (14, 48), initial reports on the effects of the anti-IL-9 monoclonal antibody enokizumab in patients was mixed (49, 50). As most of the literature in experimental models was based on acute sensitization and, in some cases, with adjuvants or adoptive transfer, we sought to address this discrepancy in a chronic adjuvant-free allergen exposure system. We found that short-term anti-IL-9 administered to chronically exposed mice with active inflammation showed little benefit. However, when it was administered to mice that were free of allergen for an extended period and then challenged, as might happen with patients that have seasonal or intermittent allergen exposure, the results were marked. Inflammation overall was decreased, with some populations including ILC2s, macrophages, and B cells, the latter requiring IL-9R in memory responses (63), being substantially affected in terms of the number or gene expression patterns. This context for IL-9 function suggests that IL-9-targeted therapies might be useful in a subset of asthma endotypes and that further investigation is warranted.

The designation of the various subsets of T_H cells is limited by assessment at a single time point and the inherent plasticity of T_H subsets in response to changing cytokine environments (64–66). Among the subsets identified, the lower expression of activation markers in T_H9 cells and the inability to find accessibility profiles unique to T_H9 cells suggested that what we termed T_H9 cells in these analyses are actually less activated T_H9rm cells. T_H2 and T_H9rm cells appeared to be more distinct based on gene expression profiles and chromatin structure. However, there could still be plasticity in these subsets that was not apparent in our data, possibly related to the heterogeneity in T_H9rm chromatin structure. As noted above, the T_H9rm cells have parallels to populations in allergic patients that are highly pathogenic, defined by multicytokine secreting patterns and the expression of ST2 (16, 28). Pathogenic T_H2 cells are found in multiple tissues including nasal polyps and esophagus (67–69). T_H2A cells are detected in patient blood highlighting the functional distinction between resident and circulating cells *in vivo* (16, 28). The separation of activity between resident and circulating T_H2 cells is based on the distinct localization of cells in the lung (70). Although IL-9 was not examined in that study, the functions of the resident T_H2 cells parallel closely with what we defined as IL-9-dependent functions *in vivo*, and it is possible that there is an overlap with the T_H9rm phenotype. Whether the resident T_H9rm cells enter the circulation is still unclear. It is possible that tissue-resident cells might exit the lung when expanded after a secondary allergen challenge. Despite this possibility, the resident IL-9-producing population still mediated inflammation when trafficking was blocked, suggesting that circulation is not essential for function in the lung.

IL-9 likely influences inflammation through several mechanisms. The cell populations in the recall model that express the most *Il9r* include CD4⁺ T cells (Tconventional and T_{reg}), ILC2s, and B cells. Our data suggest that IL-9 affects both the expansion and gene expression of these populations. Although mast cells are a known target of IL-9, in the recall model, we did not see a significant effect in this population on gene expression or cell number. In contrast, we did see changes in gene expression in interstitial macrophage populations that are a major IL-9-responsive population in a model of 6-week allergen exposure (71). We observed changes in gene expression in nonhematopoietic lung cells including mucin and other IL-13 target genes in airway epithelial cells. We saw broad, multi-population changes in the expression of secretoglobin family 1A member 1 (*Scgb1a1*), a secreted protein also known as CC10 with

anti-inflammatory properties that is predominantly expressed by respiratory epithelial cells (72, 73). In pulmonary fibrosis, the SCGB1A1⁺ MUC5B⁺ subpopulation of lung epithelial cells up-regulate expression of mucin-associated genes including *Spdef*, *Tff3*, and *Arg2* (74, 75). In addition, this subpopulation of epithelial cells promotes expression of chemoattractants for neutrophils, T cells, and monocytes (74). Consistent with these observations, in our study, *Scgb1a1* was highly expressed in the lung with isotype treatment. Blockade of IL-9 down-regulated expression of *Scgb1a1* across all cells in the lung, suggesting that a feedback mechanism fails to induce *Scgb1a1* expression as the recall response is blocked. Each of these pleiotropic effects could influence the overall amount of airway inflammation as observed in our studies. Further analysis will be needed to dissect the relative contribution of particular cell types to airway disease.

In conclusion, we showed that IL-9–secreting CD4⁺ T cells were tissue resident and mediated rapid responses to allergen challenge. IL-9 was required for allergic airway recall responses and affected multiple cell types in the allergic lung. Developing strategies to target these pathogenic IL-9–secreting Trm cells could provide therapeutic value to seasonal or intermittent exposure asthmatic patients.

MATERIALS AND METHODS

Study design

The aim of this study was to characterize IL-9–secreting T cells in allergic inflammation and determine the importance of IL-9 from T cells in allergic airway disease. Using flow cytometry in combination with intravital antibody labeling and FTY720-mediated depletion of circulating lymphocytes, we demonstrated that lung IL-9–secreting CD4⁺ T cells were tissue resident and maintained as a long-term memory population. With approaches that included using reporter mice, gene-deficient mice, and antibody treatment, we demonstrated that production of IL-9 was induced by allergen and amplified by IL-33. IL-9–secreting CD4⁺ ST2⁺ T cells were defined by scRNA-seq and scATAC-seq as producing multiple type 2 cytokines that are distinct from T_H2 cells. Through both IL-9 antibody depletion and conditional deletion of IL-9 in T cells, it was found that IL-9 was required for the recall response. Last, with scRNA-seq in the whole lung, IL-9–dependent transcription changes were found in multiple immune and structural cell populations.

Mice

C57BL/6 mice were purchased from The Jackson Laboratory. INFER mice were previously described (18). *Il9* fl/fl mice were generated by the Jackson Laboratories using Cas9-mediated targeting as outlined in fig. S6. *Il1rl1*^{-/-} mice were previously described (76). In general, experiments were performed starting with 8- to 10-week-old mice of both sexes. All experiments were performed with the approval of the Indiana University Institutional Animal Care and Use Committee.

A. fumigatus sensitization and challenge

Mice were sedated with isoflurane and sensitized intranasally to *A. fumigatus* protein extract (Greer) in PBS (25 µg/25 µl of PBS) three times per week for 6 weeks to develop a chronic response. Control mice were sensitized intranasally with PBS at these time points. To generate a memory response, mice were rested after a 6-week chronic sensitization for either 6 or 12 weeks without additional manipulation. Recall responses were induced with two doses of *A. fumigatus* protein (25 µg/25 µl of PBS) or PBS as control

separated by 24 hours with analysis 24 hours after the last challenge. An additional recall time course was completed where mice received no challenge or one recall challenge (8 hours), two recall challenges (8 and 24 hours), or three recall challenges (8, 24, and 48 hours) before analysis. In some experiments, mice received two doses of recombinant IL-33 (50 µg/25 µl of PBS, BioLegend) as a recall challenge where indicated. In some experiments, mice were treated daily with FTY720 (1 mg/kg) diluted in double-distilled H₂O delivered via intraperitoneal injection. For chronic blockade of memory T cell migration, mice were treated with FTY720 daily or vehicle control for 21 days before analysis.

IL-9, IL-13, and MHC-II blockade

To block IL-9 and IL-13 responses in the memory allergic airway disease model, 100 µg of anti-IL-9 (clone 9C1, BioXCell), anti-IL-13 (clone eBio1316H, Invitrogen), or isotype (clone C1.18.4, BioXCell) antibody was diluted either with PBS or PBS⁺ *A. fumigatus* (60-µl final volume) and delivered intranasally to mice. To block IL-9 in the chronic sensitization model, anti-IL-9 or isotype was codelivered with *A. fumigatus* during the last week (three challenges). To block MHC-II, 500 µg of anti-MHC-II (clone Y-3P, BioXCell) was delivered intravenously to mice. Antibodies including anti-MCH-II, anti-IL-9, anti-IL-13, or isotype were delivered in PBS both the 2 days before the recall challenge and during the 2 days of recall challenge.

Tissue harvest and processing

In both the chronic and memory *A. fumigatus* exposure models, circulating lymphocytes were labeled with allophycocyanin-conjugated anti-mouse CD90.2 antibody (3 µg/300 µl of PBS). Antibody was injected intravenously via the tail vein 3 min before euthanasia as described previously (77) to discriminate between circulating and tissue-resident cells. The mediastinal lymph node and spleen were collected and manually dissociated to generate single-cell suspensions. After euthanasia, the lung vascular bed was perfused through the injection of 10 ml of cold PBS via the right ventricle of the heart. Lungs were digested with collagenase A (1 mg/ml; Roche) for 45 min at 37°C followed by pressing digested lungs through a wire mesh sieve (Bellco Glass) to generate single-cell suspensions. Red blood cells were lysed using ammonium-chloride-potassium lysis buffer (Lonza). CD4⁺ T cells were isolated via magnetic bead positive selection (clone L3T4; Miltenyi Biotec). Single-cell suspensions of lung cells were stained with antibodies (table S1) to identify CD4⁺ T cells [CD4 and T cell receptor β (TCRβ)], CD8⁺ T cells (CD4⁻, CD8⁺, and TCRβ⁺), B cells (B220⁺ and CD19⁺), eosinophils (CD11b⁺, CD11c⁻, SiglecF⁺, F4/80⁺, CD45⁺, and Ly6G⁻), neutrophils (CD11b⁺, SiglecF⁻, F4/80⁻, CD45⁺, and Ly6G⁻ cells), alveolar macrophages (CD11c⁺, CD11b⁻, SiglecF⁺, F4/80⁺, CD64⁺, and Mertk⁺), interstitial macrophages (CD11b⁺, CD11c⁻, SiglecF⁻, F4/80⁺, CD64⁺, and Mertk⁺), and NK cells (CD4⁻ and NK1.1⁺).

Intracellular cytokine staining

From various tissues and time points, the frequency of cytokine-producing T cells, mast cells, and NK cells was determined by intracellular cytokine staining. Briefly, 0.2 to 1.0 × 10⁶ cells were stimulated in medium containing PMA (50 ng/ml) and ionomycin (1 µg/ml). After 4 hours, monensin (2 µM) was added to stimulated cells, and 2 hours later, cells were stained with a fixable viability dye (eBioscience) and fixed with 4% formaldehyde at room temperature for 10 min.

After fixation, cells were permeabilized with permeabilization buffer (eBioscience) and stained for intracellular cytokines (table S1) in the same buffer. In flow cytometry analysis, gates of cytokine positive populations were determined on the basis of unstimulated or naïve cell controls.

Isolation and detection of ILC2 population in the lung

The ILC2 population in the whole lung was identified as Lineage⁻ (Lin⁻), CD45.2⁺, CD90.2 (Thy1.2)⁺, Sca-1⁺, Klrg-1⁺, and ST2⁺. In addition to allergic airway models to detect ILC2 cytokine production, *Il9 fl/fl Cd4⁻cre⁻* and *Il9 fl/fl Cd4⁻cre⁺* mice were treated intranasally with 0.5 µg of IL-33 for 3 days. On day 4, lungs were harvested and processed for detection of ILC2 population. For detection of IL-9-secreting ILC2s, single-cell suspension of lung cells was stimulated with IL-33 (50 ng/ml) for 6 hours and treated with monensin for 2 hours. Surface and intracellular staining was performed as described (table S1).

In vitro cell culture

Differentiation of T_H9 cells from naïve CD4 T cells was performed as described (78). Briefly, splenic CD4⁺ CD62L⁺ T cells were isolated using magnetic separation (Miltenyi), activated with anti-CD3 (BioXCell) and anti-CD28 (BioXCell), and cultured with human TGF-β1 (2 ng/ml; PeproTech), IL-4 (20 ng/ml; PeproTech), and anti-IFN-γ (10 µg/ml; BioXCell) for 5 days. For isolation of peritoneal mast cells, peritoneal cells were washed from the peritoneal cavity using peritoneal lavage. Suspension of peritoneal cells was centrifuged at 300g and resuspended in RPMI 1640 medium supplemented with 10% fetal calf serum, 1% penicillin-streptomycin, 1% L-glutamine, 1% sodium pyruvate, 1% of 10 mM Hepes, IL-3 (30 ng/ml), and stem cell factor (60 ng/ml) (mast cell medium). Cells were cultured in 5% CO₂ at 37°C. After 24 hours of culture, nonadherent cells were transferred to a new cell culture dish and were further cultured for an additional 5 days. On day 7, cells were washed with PBS and resuspended in mast cell medium without the addition of cytokines. Mast cells were identified as CD117⁺ and FcεRIα⁺.

Airway resistance

One day after final intranasal challenge, mice were given increasing doses of intratracheal methacholine. Readings were obtained at baseline and after exposure to increasing doses of aerosolized methacholine for up to 100 mg/ml. Data were collected for 5 min after 3 min of inhalation, and average values were expressed as airway resistance. The airway response was measured for up to 45 min. Airway resistance was measured using a ventilator (Elan Series Mouse RC Site, Buxco Electronics) and BioSystem XA software (Buxco Electronics).

Cytokine assay

CD4⁺ T cells were sorted from the lungs of *A. fumigatus*-challenged mice by magnetic CD4 antibody-mediated positive selection (Miltenyi). The 50,000 purified CD4⁺ T cells were cocultured with an equal number of CD11c⁺ antigen-presenting cells [purified by CD11c antibody-mediated positive selection (Miltenyi)] in the presence of either BSA, *A. fumigatus* (100 mg/ml; Greer), *A. alternata* (100 mg/ml; Greer), or HDM (100 mg/ml; Greer) for 72 hours in RPMI 1640 complete medium in a 96-well U-bottom plate. In some experiment, additional controls and innate cytokines (50 ng/ml) were added to the coculture. IL-9 was measured by enzyme-linked immunosorbent assay (ELISA) MAX Deluxe Set Mouse IL-9 (BioLegend).

Histology

Lung tissues were preserved in fixative 10% buffered formalin at room temperature. After 1 week, formalin was replaced with 70% ethanol and stored at room temperature until processing. All samples were submitted and processed with hematoxylin and eosin (H&E) and trichrome staining by the Indiana University (IU) Histology Core Facility. Fixed samples were processed for paraffin embedding in blocks and cut by rotary microtome into 5-µm-thick sections. Sections were mounted on glass slides and stained. For H&E staining, slides were stained following the LINISTAIN GLX linear stainer method with slides undergoing washes in xylenes, ethanol, Harris' hematoxylin (Surgipath), 70% ethanol + HCl, 0.3% ammonium hydroxide + water, and eosin (Surgipath). For trichrome staining, deparaffinized slides were fixed in Bouin's solution (37% formaldehyde + picric acid + glacial acetic acid) and microwaved on high for 1 min. Slides were stained with Gill's no. 3 hematoxylin (Surgipath), Scott solution (0.2% sodium bicarbonate + 2% magnesium sulfate), Beirich Scarlet-Acid Fuchsin Solution (Sigma-Aldrich), phosphotungstic/phosphomolybdic acid (Sigma-Aldrich), and aniline blue solution (Sigma-Aldrich).

Immunofluorescence staining

Lobes of the lung from memory *A. fumigatus* exposure model using INFER IL-9 reporter mice were snap-frozen in liquid nitrogen after being perfused with cold 1× PBS buffer. Lung tissues were briefly thawed, perfused with optimal cutting temperature (OCT) compound by injection into the tissue, and embedded in OCT compound in metal molds under a slurry of dry ice and methanol. The frozen OCT compound embedded tissue samples were further sectioned at the IU's Histology Core Facility. For immunofluorescence staining, sections were thawed at room temperature for 1 hour followed by three 5-min washes with 1× PBS. Tissue sections were blocked with a blocking buffer (Protein Block Serum-Free, Dako, X0909) in a humidity chamber for 1 hour at room temperature. The sections were then washed twice with 1× PBS and incubated overnight at 4°C with the rat anti-CD4 primary antibody diluted (1:500) in antibody diluent (Dako, S3022). Tissue sections were washed three times in 1× PBS and incubated with the secondary antibody (goat anti-rat IgG AF568, Invitrogen, A-11077) for 1 hour at room temperature in the humidity chamber. The sections were washed twice with 1× PBS and stained with 4',6-diamidino-2-phenylindole at room temperature for 3 min. Sections were washed three times in 1× PBS, dried, and mounted with EverBrite mounting media (Biotium, 23003). Images were acquired on an LSM700 or 800 confocal microscope (Zeiss) using a 10×/0.3 numerical aperture (NA) or 20×/0.8 NA objective. For enumeration of GFP⁺ CD90.2⁻ CD4 T cells in the lung tissue sections, single blinded cell counts from six individuals were averaged across four field-of-lung tissue sections before and at 24 hours after recall challenge.

Real-time PCR

RNA was harvested from large bulk populations at the indicated time points in TRIzol reagent (Life Technologies). RNA was harvested from smaller cell populations (under 400,000 cells) using an RNeasy plus mini kit (Qiagen). cDNA was produced by reverse transcribing mRNA via the qScript cDNA Synthesis Kit (Quantabio). Real-time polymerase chain reaction (PCR) was carried out with TaqMan primers (Life Technologies) using a 7500 Fast-PCR machine (Life Technologies).

Sample preparation for scRNA-seq and ATAC-seq

Single-cell suspensions of mouse lung cells were obtained from memory *A. fumigatus* exposure model with anti-IL-9 or isotype blockade ($n = 3$). Dead cells were removed using the MACS Dead Cell removal kit (Miltenyi) following the manufacturer's instructions. To analyze IL-9-secreting population in the recall model, lung cells were stained with CD4 and ST2 antibodies for 30 min at 4°C. ST2⁺ CD4⁺ T cells and ST2⁻ CD4 T cells were sorted at the IU flow cytometry core and pooled from individual mice ($n = 2$ per replicate). Cellular concentration was determined using a Countess II FL Automated Cell Counter and adjusted to $\sim 7 \times 10^5$ cells/ml (700 cells/ μ l) before single-cell analysis for RNA-seq and ATAC-seq.

scRNA-seq and analysis

Library preparation for scRNA-seq was performed using the following kits: Chromium Single-Cell 3' Library and Gel Bead Kit V3, 4 rxns PN-120267; Chromium Single-Cell A Chip Kit, 16 rxns PN-1000009; and Chromium i7 Multiplex Kit, 96 rxns PN-120262. Twenty-eight base pairs (bp) of cell barcode and unique molecular indices (UMIs) sequences and 91-bp RNA reads were generated with Illumina NovaSeq 6000 at the Indiana University School of Medicine Center for Molecular Genomics. CellRanger 3.0.2 was used to process the raw sequence data generated. Briefly, CellRanger used bcl2fastq to demultiplex raw base sequence calls generated from the sequencer into sample specific FASTQ files. The FASTQ files were then aligned to the mouse reference genome mm10 with RNA-seq aligner STAR. The aligned reads were traced back to individual cells, and the gene expression level of individual genes was quantified on the basis of the number of UMIs detected in each cell. The filtered feature-cell barcode matrices generated by CellRanger were used for further analysis. For each sample, the mean reads per cell were at least 35,000 bp with a median of at least 1645 unique genes per cell. A representative sample from each condition [similar trends in differentially expressed genes (DEGs) were observed in replicates] that were run at the same time to avoid batch effects was selected on the basis of sequencing depth to be used for further downstream analysis as described below.

The R package Seurat version 3.2.1 and Seurat version 4 (79–81) were used for the following analyses: cell type/state discovery with graph-based clustering, cell cluster marker gene identification, various visualization, and differential gene expression. Quality control (QC) analysis in Seurat was used to determine the parameters used for excluding low-quality cells. Low-quality cells were excluded with the following criteria: cells with unique feature/gene counts over 5000 or less than 500 or >10% mitochondrial genes. Clusters were identified with the Seurat functions "FindNeighbors" and "FindClusters" using a resolution of 0.75 and 36 principal components. UMAP was used for dimensional reduction and visualization. For cluster identification in mouse whole-lung samples, Seurat function FindAllMarkers was used. For further classification of ST2⁺ CD4⁺ T cells samples, T helper populations including T_H9rm, T_H2, and T_H9 were further identified on the basis of raw read counts of *Il9*, *Il5*, and *Il13*. T_H9rm cells were defined with *Il5* and *Il13* counts greater than or equal to 3 and *Il9* counts greater than 0. T_H2 cells were defined with *Il5* and *Il13* counts greater than or equal to 3 and *Il9* counts equal to 0. T_H9 cells were defined with *Il5* and *Il13* counts less than 3 and *Il9* counts greater than 0. These cell subset designations were based on iterating from integers 0 through 5 for each combination of *Il5*, *Il13*, and *Il9* and producing a corresponding unsupervised UMAP until a

sufficiently segregated clustering scheme was produced. Differential gene expression analysis was performed with Seurat function FindMarkers using Wilcoxon rank sum test. Seurat in-built visualization tools were used for plotting heatmaps, violin plots, feature plots, dot plots, and UMAPs. An R package called EnhancedVolcanoPlots was used to plot volcano plots, where significantly differentially expressed genes were identified as $P < 0.05$ and \log_2 fold change > 0.25 . Monocle 3 package (82) was used to construct the lineage trajectory for a subset of the ST2⁺ CD4⁺ T cell samples (naïve, T cells, and type 2 T_H). Preprocessing and dimensional reduction were performed as previously mentioned using a Seurat object after which the dimensional embeddings were imported to Monocle3 to manually create the associated cell dataset object. A principal graph was fitted to the cell landscape to traverse the clusters before ordering the cells along a trajectory of pseudotime. The pseudotime root was specified as the naïve cell cluster based on previously assessed naïve cell markers (high *Sell* and *Ccr7*, low *Cd44*). We then plotted some transcription factors and cytokines as a function of pseudotime using in-built functions.

scATAC-seq and analysis

The Chromium single-cell ATAC Kit was used for library preparation. The scATAC-seq experiment was conducted using the Chromium single-cell system (10x Genomics Inc) and the NovaSeq 6000 sequencer (Illumina Inc). Sixteen base pairs of cell barcode and 49-bp paired-end reads were generated with Illumina NovaSeq 6000 at the Center for Medical Genomics of Indiana University School of Medicine. CellRanger-atac v1.1.0 was used to process the raw sequence data generated. The filtered barcode-peak matrices and fragment file generated by CellRanger were used for further analysis. At least 11,000 cells were analyzed, with a median of 10,282 fragments per nucleus. The R package Seurat version 3.2.1 (79–81) and Signac 0.1.6 were used for the following analyses.

QC metrics calculations included nucleosome banding pattern (ratio of mononucleosomal to nucleosome-free fragments), transcriptional start site (TSS) enrichment score (based on the ratio of fragments centered at the TSS to fragments in TSS-flanking regions), total number of fragments in peaks, fraction of fragments in peaks, and ratio reads in "blacklist" sites. Cells that were considered outliers from these QC metrics were removed from further analysis. Data were normalized with term frequency-inverse document frequency (TF-IDF) normalization. Dimensional reduction for performed using a singular value decomposition on the TD-IDF-normalized matrix. Nonlinear dimension reduction and clustering were performed for graph-based clustering and nonlinear dimensional reduction for visualization (functions RunUMAP, FindNeighbors, and FindClusters from the Seurat package). Preprocessed scRNA-seq Seurat object for ST2⁺ CD4⁺ T cells sample was integrated with scATAC-seq seurat object by performing cross-modality integration and label transfer (functions: FindTransferAnchors and TranferData). Cell clusters including T_H2 and T_H9rm were further identified on the basis of gene activity for *Il9*, *Il5*, and *Il13*. Differentially accessible peaks and active loci were analyzed using FindMarkers function within Seurat package, and enriched motifs were identified using ChromVar R package.

Statistics and data analysis

All statistics were done using Prism software version 7 (GraphPad). Student's unpaired two-tailed *t* test, one-way analysis of variance

(ANOVA) with a post hoc Tukey test, and two-way ANOVA with a post hoc Tukey test were used for comparison to generate *P* values as described in each figure legend. Significance was identified with **P* < 0.05, ***P* < 0.01, ****P* < 0.001, and *****P* < 0.0001. Flow cytometry data were collected using a Nxt Attune flow cytometer (Life Technologies) and was analyzed using FloJo version 10 (Tree Star).

SUPPLEMENTARY MATERIALS

www.science.org/doi/10.1126/scimmunol.abg9296

Figs. S1 to S8

Table S1

Data files S1 to S6

[View/request a protocol for this paper from Bio-protocol.](#)

REFERENCES AND NOTES

- R. M. Locksley, Asthma and allergic inflammation. *Cell* **140**, 777–783 (2010).
- D. S. Robinson, Q. Hamid, S. Ying, A. Tsicopoulos, J. Barkans, A. M. Bentley, C. Corrigan, S. R. Durham, A. B. Kay, Predominant TH2-like Bronchoalveolar T-lymphocyte population in atopic asthma. *N. Engl. J. Med.* **326**, 298–304 (1992).
- S. T. Holgate, Innate and adaptive immune responses in asthma. *Nat. Med.* **18**, 673–683 (2012).
- J. R. Crosby, H. H. Shen, M. T. Borchers, J. P. Justice, T. Ansary, J. J. Lee, N. A. Lee, Ectopic expression of IL-5 identifies an additional CD4+ T cell mechanism of airway eosinophil recruitment. *Am. J. Physiol. Lung Cell. Mol. Physiol.* **282**, L99–L108 (2002).
- S. M. Pope, E. B. Brandt, A. Mishra, S. P. Hogan, N. Zimmermann, K. I. Matthaei, P. S. Foster, M. E. Rothenberg, IL-13 induces eosinophil recruitment into the lung by an IL-5- and eotaxin-dependent mechanism. *J. Allergy Clin. Immunol.* **108**, 594–601 (2001).
- S. Sur, G. J. Gleich, K. P. Offord, M. C. Swanson, T. Ohnishi, L. B. Martin, J. M. Wagner, D. A. Weiler, L. W. Hunt, Allergen challenge in asthma: Association of eosinophils and lymphocytes with interleukin-5. *Allergy* **50**, 891–898 (1995).
- L. M. Teran, Chemokines and IL-5: Major players of eosinophil recruitment in asthma. *Clin. Exp. Allergy* **29**, 287–290 (1999).
- L. Cohn, R. J. Homer, N. Niu, K. Bottomly, T Helper 1 cells and interferon γ regulate allergic airway inflammation and mucus production. *J. Exp. Med.* **190**, 1309–1318 (1999).
- M. Wills-Karp, Immunologic basis of antigen-induced airway hyperresponsiveness. *Annu. Rev. Immunol.* **17**, 255–281 (1999).
- M. L. Fajt, S. E. Wenzel, Asthma phenotypes and the use of biologic medications in asthma and allergic disease: The next steps toward personalized care. *J. Allergy Clin. Immunol.* **135**, 299–310 (2015).
- M. H. Kaplan, M. M. Hufford, M. R. Olson, The development and in vivo function of T helper 9 cells. *Nat. Rev. Immunol.* **15**, 295–307 (2015).
- H.-C. Chang, S. Sehra, R. Goswami, W. Yao, Q. Yu, G. L. Stritesky, R. Jabeen, C. McKinley, A.-N. Ahyi, L. Han, E. T. Nguyen, M. J. Robertson, N. B. Perumal, R. S. Tepper, S. L. Nutt, M. H. Kaplan, The transcription factor PU.1 is required for the development of IL-9-producing T cells and allergic inflammation. *Nat. Immunol.* **11**, 527–534 (2010).
- C. P. Jones, L. G. Gregory, B. Causton, G. A. Campbell, C. M. Lloyd, Activin A and TGF- β promote T_H9 cell-mediated pulmonary allergic pathology. *J. Allergy Clin. Immunol.* **129**, 1000–10.e3 (2012).
- W. Yao, Y. Zhang, R. Jabeen, E. T. Nguyen, D. S. Wilkes, R. S. Tepper, M. H. Kaplan, B. Zhou, Interleukin-9 is required for allergic airway inflammation mediated by the cytokine TSLP. *Immunity* **38**, 360–372 (2013).
- S. Devos, F. Cormont, S. Vrtala, E. Hooghe-Peters, F. Pirson, J. Van Snick, Allergen-induced interleukin-9 production in vitro: Correlation with atopy in human adults and comparison with interleukin-5 and interleukin-13. *Clin. Exp. Allergy* **36**, 174–182 (2006).
- G. Seumois, C. Ramírez-Suárez, B. J. Schmiedel, S. Liang, B. Peters, A. Sette, P. Vijayanand, Single-cell transcriptomic analysis of allergen-specific T cells in allergy and asthma. *Sci. Immunol.* **5**, eaba6087 (2020).
- J. Kearley, J. S. Erjefalt, C. Andersson, E. Benjamin, C. P. Jones, A. Robichaud, S. Pegorier, Y. Brewah, T. J. Burwell, L. Bjermer, P. A. Kiener, R. Kolbeck, C. M. Lloyd, A. J. Coyle, A. A. Humbles, IL-9 Governs allergen-induced mast cell numbers in the lung and chronic remodeling of the airways. *Am. J. Respir. Crit. Care Med.* **183**, 865–875 (2011).
- P. Licona-Limón, J. Henao-Mejía, A. U. Temann, N. Gagliani, I. Licona-Limón, H. Ishigame, L. Hao, D. R. Herbert, R. A. Flavell, Th9 cells drive host immunity against gastrointestinal worm infection. *Immunity* **39**, 744–757 (2013).
- U.-A. Temann, G. P. Geba, J. A. Rankin, R. A. Flavell, Expression of interleukin 9 in the lungs of transgenic mice causes airway inflammation, mast cell hyperplasia, and bronchial hyperresponsiveness. *J. Exp. Med.* **188**, 1307–1320 (1998).
- M. C. Altman, E. Whalen, A. Togias, G. T. O'Connor, L. B. Bacharier, G. R. Bloomberg, M. Kattan, R. A. Wood, S. Presnell, P. LeBeau, K. Jaffee, C. M. Visness, W. W. Busse, J. E. Gern, Allergen-induced activation of natural killer cells represents an early-life immune response in the development of allergic asthma. *J. Allergy Clin. Immunol.* **142**, 1856–1866 (2018).
- M. Richard, R. K. Gencis, N. E. Humphreys, J.-C. Renaud, J. Van Snick, Anti-IL-9 vaccination prevents worm expulsion and blood eosinophilia in *Trichuris muris*-infected mice. *Proc. Natl. Acad. Sci.* **97**, 767–772 (2000).
- M. J. Townsend, P. G. Fallon, D. J. Matthews, P. Smith, H. E. Jolin, A. N. J. McKenzie, IL-9-deficient mice establish fundamental roles for IL-9 in pulmonary mastocytosis and goblet cell hyperplasia but not T cell development. *Immunity* **13**, 573–583 (2000).
- T. Nakayama, K. Hirahara, A. Onodera, Y. Endo, H. Hosokawa, K. Shinoda, D. J. Tumes, Y. Okamoto, Th2 cells in health and disease. *Annu. Rev. Immunol.* **35**, 53–84 (2017).
- D. J. Cousins, T. H. Lee, D. Z. Staynov, Cytokine coexpression during human Th1/Th2 cell differentiation: Direct evidence for coordinated expression of Th2 cytokines. *J. Immunol.* **169**, 2498–2506 (2002).
- S. A. Islam, M. F. Ling, J. Leung, W. G. Shreffler, A. D. Luster, Identification of human CCR8 as a CCL18 receptor. *J. Exp. Med.* **210**, 1889–1898 (2013).
- A. Mitson-Salazar, C. Prusin, Pathogenic effector Th2 cells in allergic eosinophilic inflammatory disease. *Front. Med.* **4**, 165 (2017).
- B. Upadhyaya, Y. Yin, B. J. Hill, D. C. Douek, C. Prusin, Hierarchical IL-5 expression defines a subpopulation of highly differentiated human Th2 cells. *J. Immunol.* **187**, 3111–3120 (2011).
- E. Wambre, V. Bajzik, J. H. DeLong, K. O'Brien, Q.-A. Nguyen, C. Speake, V. H. Gersuk, H. A. DeBerg, E. Whalen, C. Ni, M. Farrington, D. Jeong, D. Robinson, P. S. Linsley, B. P. Vickery, W. W. Kwok, A phenotypically and functionally distinct human T_H2 cell subpopulation is associated with allergic disorders. *Sci. Transl. Med.* **9**, eaam9171 (2017).
- C. Micossé, L. von Meyenn, O. Steck, E. Kipfer, C. Adam, C. Simillion, S. M. Seyed Jafari, P. Olah, N. Yawlkar, D. Simon, L. Borradori, S. Kuchen, D. Yerly, B. Homey, C. Conrad, B. Snijder, M. Schmidt, C. Schlapbach, Human “T_H9” cells are a subpopulation of PPAR- γ ⁺ T_H2 cells. *Sci. Immunol.* **4**, eaat5943 (2019).
- E. M. Steinert, J. M. Schenkel, K. A. Fraser, L. K. Beura, L. S. Manlove, B. Z. Iggyártó, P. J. Southern, D. Masopust, Quantifying memory CD8 T cells reveals regionalization of immunosurveillance. *Cell* **161**, 737–749 (2015).
- B. V. Kumar, W. Ma, M. Miron, T. Granot, R. S. Guyer, D. J. Carpenter, T. Senda, X. Sun, S.-H. Ho, H. Lerner, A. L. Friedman, Y. Shen, D. L. Farber, Human tissue-resident memory T cells are defined by core transcriptional and functional signatures in lymphoid and mucosal sites. *Cell Rep.* **20**, 2921–2934 (2017).
- B. D. Hondowicz, D. An, J. M. Schenkel, K. S. Kim, H. R. Steach, A. T. Krishnamurti, G. J. Keitany, E. N. Garza, K. A. Fraser, J. J. Moon, W. A. Altemeier, D. Masopust, M. Pepper, Interleukin-2-dependent allergen-specific tissue-resident memory cells drive asthma. *Immunity* **44**, 155–166 (2016).
- K. L. Reagin, K. D. Klonowski, Incomplete memories: The natural suppression of tissue-resident memory CD8 T cells in the lung. *Front. Immunol.* **9**, 17–17 (2018).
- D. L. Turner, M. Goldklang, F. Cvetkovski, D. Paik, J. Trischler, J. Barahona, M. Cao, R. Dave, N. Tanna, J. M. D'Armiesto, D. L. Farber, Biased generation and *in situ* activation of lung tissue-resident memory CD4 T cells in the pathogenesis of allergic asthma. *J. Immunol.* **200**, 1561–1569 (2018).
- J. Kerzerho, H. Maazi, A. O. Speak, N. Szely, V. Lombardi, B. Khoo, S. Geryak, J. Lam, P. Soroosh, J. Van Snick, O. Akbari, Programmed cell death ligand 2 regulates TH9 differentiation and induction of chronic airway hyperreactivity. *J. Allergy Clin. Immunol.* **131**, 1048–1057.e2 (2013).
- J. R. Teijaro, D. Turner, Q. Pham, E. J. Wherry, L. Lefrançois, D. L. Farber, Cutting Edge: Tissue-retentive lung memory CD4 T cells mediate optimal protection to respiratory virus infection. *J. Immunol.* **187**, 5510–5514 (2011).
- D. L. Turner, K. L. Bickham, J. J. Thome, C. Y. Kim, F. D'Ovidio, E. J. Wherry, D. L. Farber, Lung niches for the generation and maintenance of tissue-resident memory T cells. *Mucosal Immunol.* **7**, 501–510 (2014).
- S. Suzuki, S. Enosawa, T. Kakefuda, T. Shinomiya, M. Amari, S. Naoe, Y. Hoshino, K. Chiba, A novel immunosuppressant, FTY720, with a unique mechanism of action, induces long-term graft acceptance in rat and dog allograft transplantation. *Transplantation* **61**, 200–205 (1996).
- Y. Yanagawa, K. Sugahara, H. Kataoka, T. Kawaguchi, Y. Masubuchi, K. Chiba, FTY720, a novel immunosuppressant, induces sequestration of circulating mature lymphocytes by acceleration of lymphocyte homing in rats. II. FTY720 prolongs skin allograft survival by decreasing T cell infiltration into grafts but not cytokine production *in vivo*. *J. Immunol.* **160**, 5493–5499 (1998).
- H. Yagi, R. Kamba, K. Chiba, H. Soga, K. Yaguchi, M. Nakamura, T. Itoh, Immunosuppressant FTY720 inhibits thymocyte emigration. *Eur. J. Immunol.* **30**, 1435–1444 (2000).
- C. Wilhelm, K. Hirota, B. Stieglitz, J. Van Snick, M. Tolaini, K. Lahl, T. Sparwasser, H. Helmby, B. Stockinger, An IL-9 fate reporter demonstrates the induction

- of an innate IL-9 response in lung inflammation. *Nat. Immunol.* **12**, 1071–1077 (2011).
42. I. Martinez-Gonzalez, L. Mathä, C. A. Steer, M. Ghaedi, G. F. T. Poon, F. Takei, Allergen-experienced group 2 innate lymphoid cells acquire memory-like properties and enhance allergic lung inflammation. *Immunity* **45**, 198–208 (2016).
 43. R. Kharwadkar, B. J. Ulrich, A. Abdul Qayum, B. Koh, P. Licona-Limón, R. A. Flavell, M. H. Kaplan, Expression efficiency of multiple *IIL9* reporter alleles is determined by cell lineage. *ImmunoHorizons* **4**, 282–291 (2020).
 44. C. Schlapbach, A. Gehad, C. Yang, R. Watanabe, E. Guenova, J. E. Teague, L. Campbell, N. Yawalkar, T. S. Kupper, R. A. Clark, Human T_H9 cells are skin-tropic and have autocrine and paracrine proinflammatory capacity. *Sci. Transl. Med.* **6**, 219ra8 (2014).
 45. F. Alvarez, J. H. Fritz, C. A. Piccirillo, Pleiotropic effects of IL-33 on CD4+ T cell differentiation and effector functions. *Front. Immunol.* **10**, 522 (2019).
 46. L. Guo, Y. Huang, X. Chen, J. Hu-Li, J. F. Urban, W. E. Paul, Innate immunological function of TH2 cells in vivo. *Nat. Immunol.* **16**, 1051–1059 (2015).
 47. P. Li, R. Spolski, W. Liao, W. J. Leonard, Complex interactions of transcription factors in mediating cytokine biology in T cells. *Immunol. Rev.* **261**, 141–156 (2014).
 48. V. Staudt, E. Bothur, M. Klein, K. Lingnau, S. Reuter, N. Grebe, B. Gerlitzki, M. Hoffmann, A. Ulges, C. Taube, N. Dehzad, M. Becker, M. Stassen, A. Steinborn, M. Lohoff, H. Schild, E. Schmitt, T. Bopp, Interferon-regulatory factor 4 is essential for the developmental program of T helper 9 cells. *Immunity* **33**, 192–202 (2010).
 49. C. K. Oh, R. Leigh, K. K. McLaurin, K. Kim, M. Hultquist, N. A. Molfino, A randomized, controlled trial to evaluate the effect of an anti-interleukin-9 monoclonal antibody in adults with uncontrolled asthma. *Respir. Res.* **14**, 93 (2013).
 50. B. White, F. Leon, W. White, G. Robbie, Two first-in-human, open-label, phase I dose-escalation safety trials of MEDI-528, a monoclonal antibody against interleukin-9, in healthy adult volunteers. *Clin. Ther.* **31**, 728–740 (2009).
 51. D. J. Hodson, M. L. Janas, A. Galloway, S. E. Bell, S. Andrews, C. M. Li, R. Pannell, C. W. Siebel, H. R. MacDonald, K. De Keersmaecker, A. A. Ferrando, G. Grutz, M. Turner, Deletion of the RNA-binding proteins ZFP36L1 and ZFP36L2 leads to perturbed thymic development and T lymphoblastic leukemia. *Nat. Immunol.* **11**, 717–724 (2010).
 52. K. U. Vogel, L. S. Bell, A. Galloway, H. Ahlfors, M. Turner, The RNA-binding proteins Zfp36l1 and Zfp36l2 enforce the thymic β-selection checkpoint by limiting DNA damage response signaling and cell cycle progression. *J. Immunol.* **197**, 2673–2685 (2016).
 53. A. Saveliev, S. E. Bell, M. Turner, Efficient homing of antibody-secreting cells to the bone marrow requires RNA-binding protein ZFP36L1. *J. Exp. Med.* **218**, e20200504 (2020).
 54. N. D. Jackson, J. L. Everman, M. Chioccioli, L. Feriani, K. C. Goldfarb, Muren, S. P. Sajuthi, C. L. Rios, R. Powell, M. Armstrong, J. Gomez, C. Michel, C. Eng, S. S. Oh, J. Rodriguez-Santana, P. Cicuta, N. Reisdorph, E. G. Burchard, M. A. Seibold, Single-cell and population transcriptomics reveal pan-epithelial remodeling in type 2-high asthma. *Cell Rep.* **32**, 107872 (2020).
 55. L. Zhu, L. An, D. Ran, R. Lizarraga, C. Bondy, X. Zhou, R. W. Harper, S.-Y. Liao, Y. Chen, The club cell marker SCGB1A1 downstream of FOXA2 is reduced in asthma. *Am. J. Respir. Cell Mol. Biol.* **60**, 695–704 (2018).
 56. P. Rajavelu, G. Chen, Y. Xu, J. A. Kitzmiller, T. R. Korfhagen, J. A. Whitsett, Airway epithelial SPDEF integrates goblet cell differentiation and pulmonary Th2 inflammation. *J. Clin. Invest.* **125**, 2021–2031 (2015).
 57. G. Chen, T. R. Korfhagen, Y. Xu, J. Kitzmiller, S. E. Wert, Y. Maeda, A. Gregorieff, H. Clevers, J. A. Whitsett, SPDEF is required for mouse pulmonary goblet cell differentiation and regulates a network of genes associated with mucus production. *J. Clin. Invest.* **119**, 2914–2924 (2009).
 58. J. Zhao, B. Maskrey, S. Balzar, K. Chibana, A. Mustovich, H. Hu, J. B. Trudeau, V. O'Donnell, S. E. Wenzel, Interleukin-13-induced MUC5AC is regulated by 15-lipoxygenase 1 pathway in human bronchial epithelial cells. *Am. J. Respir. Crit. Care Med.* **179**, 782–790 (2009).
 59. X. Tang, X. J. Liu, C. Tian, Q. Su, Y. Lei, Q. Wu, Y. He, J. A. Whitsett, F. Luo, Foxa2 regulates leukotrienes to inhibit Th2-mediated pulmonary inflammation. *Am. J. Respir. Cell Mol. Biol.* **49**, 960–970 (2013).
 60. C. Tan, M. K. Aziz, J. D. Lovaas, B. P. Vistica, G. Shi, E. F. Wawrousek, I. Gery, Antigen-specific Th9 cells exhibit uniqueness in their kinetics of cytokine production and short retention at the inflammatory site. *J. Immunol.* **185**, 6795–6801 (2010).
 61. E. Cano-Gamez, B. Soskic, T. I. Roumeliotis, E. So, D. J. Smyth, M. Baldighi, D. Willé, N. Nakic, J. Esparza-Gordillo, C. G. Larminie, P. G. Bronson, D. F. Tough, W. C. Rowan, J. S. Choudhary, G. Trynka, Single-cell transcriptomics identifies an effectorness gradient shaping the response of CD4+ T cells to cytokines. *Nat. Commun.* **11**, 1801 (2020).
 62. C. A. Tibbitt, J. M. Stark, L. Martens, J. Ma, J. E. Mold, K. Deswarte, G. Oliynyk, X. Feng, B. N. Lambrecht, P. De Bleser, S. Nylen, H. Hammad, M. Arsenian Henriksson, Y. Saeyns, J. M. Coquet, Single-cell RNA sequencing of the T helper cell response to house dust mites defines a distinct gene expression signature in airway Th2 cells. *Immunity* **51**, 169–184.e5 (2019).
 63. S. Takatsuka, H. Yamada, K. Haniuda, H. Saruwatari, M. Ichihashi, J.-C. Renaud, D. Kitamura, IL-9 receptor signaling in memory B cells regulates humoral recall responses. *Nat. Immunol.* **19**, 1025–1034 (2018).
 64. S. Tuzlak, A. S. Dejean, M. Iannaccone, F. J. Quintana, A. Waisman, F. Ginhoux, T. Korn, B. Becher, Repositioning TH cell polarization from single cytokines to complex help. *Nat. Immunol.* **22**, 1210–1217 (2021).
 65. L. Tortola, A. Jacobs, L. Pohlmeier, F.-J. Obermair, F. Ampenberger, B. Bodenmiller, M. Kopf, High-dimensional T helper cell profiling reveals a broad diversity of stably committed effector states and uncovers interlineage relationships. *Immunity* **53**, 597–613.e6 (2020).
 66. J. J. O'Shea, W. E. Paul, Mechanisms underlying lineage commitment and plasticity of helper CD4+ T cells. *Science* **327**, 1098–1102 (2010).
 67. K. Hirahara, A. Aoki, M. Kiuchi, T. Nakayama, Memory-type pathogenic TH2 cells and ILC2s in type 2 allergic inflammation. *J. Allergy Clin. Immunol.* **147**, 2063–2066 (2021).
 68. D. M. Morgan, B. Ruiter, N. P. Smith, A. A. Tu, B. Monian, B. E. Stone, N. Virk-Hundal, Q. Yuan, W. G. Shreffler, J. C. Love, Clonally expanded, GPR15-expressing pathogenic effector T_H2 cells are associated with eosinophilic esophagitis. *Sci. Immunol.* **6**, eabi5586 (2021).
 69. J. Ma, C. A. Tibbitt, S. K. Georén, M. Christian, B. Murrell, L.-O. Cardell, C. Bachert, J. M. Coquet, Single-cell analysis pinpoints distinct populations of cytotoxic CD4+ T cells and an IL-10⁺CD109⁺ T_H2 cell population in nasal polyps. *Sci. Immunol.* **6**, eabg6356 (2021).
 70. R. A. Rahimi, K. Nepal, M. Cetinbas, R. I. Sadreyev, A. D. Luster, Distinct functions of tissue-resident and circulating memory Th2 cells in allergic airway disease. *J. Exp. Med.* **217**, e20190865 (2020).
 71. Y. Fu, J. Wang, B. Zhou, A. Pajulas, H. Gao, B. Ramdas, B. Koh, B. Ulrich, S. Yang, R. Kapur, J.-C. Renaud, S. Paczesny, Y. Liu, R. Tighe, P. Licona-Limon, R. Flavell, S. Takatsuka, D. Kitamura, R. Tepper, J. Sun, M. Kaplan, An IL-9-pulmonary macrophage axis defines the allergic lung inflammatory environment. *Sci. Immunol.* **7**, eabi9768 (2022).
 72. G. Singh, S. L. Katyal, Clara Cells and Clara Cell 10 kD Protein (CC10). *Am. J. Respir. Cell Mol. Biol.* **17**, 141–143 (1997).
 73. E. Tokita, T. Tanabe, K. Asano, H. Suzuki, B. K. Rubin, Club cell 10-kDa protein attenuates airway mucus hypersecretion and inflammation. *Eur. Respir. J.* **44**, 1002–1010 (2014).
 74. W.-L. Zuo, M. R. Rostami, M. LeBlanc, R. J. Kaner, S. L. O'Beirne, J. G. Mezey, P. L. Leopold, K. Quast, S. Visvanathan, J. S. Fine, M. J. Thomas, R. G. Crystal, Dysregulation of club cell biology in idiopathic pulmonary fibrosis. *PLOS ONE* **15**, e0237529 (2020).
 75. I. Buendía-Roldán, V. Ruiz, P. Sierra, E. Montes, R. Ramírez, A. Vega, A. Salgado, M. H. Vargas, M. Mejía, A. Pardo, M. Selman, Increased expression of CC16 in patients with idiopathic pulmonary fibrosis. *PLOS ONE* **11**, e0168552 (2016).
 76. M. J. Townsend, P. G. Fallon, D. J. Matthews, H. E. Jolin, A. N. J. McKenzie, T1/St2-deficient mice demonstrate the importance of T1/St2 in developing primary T helper cell type 2 responses. *J. Exp. Med.* **191**, 1069–1076 (2000).
 77. K. G. Anderson, K. Mayer-Barber, H. Sung, L. Beura, B. R. James, J. J. Taylor, L. Qunaj, T. S. Griffith, V. Vezy, D. L. Barber, D. Masopust, Intravascular staining for discrimination of vascular and tissue leukocytes. *Nat. Protoc.* **9**, 209–222 (2014).
 78. Y. Fu, B. Koh, M. Kuwahara, B. J. Ulrich, R. Kharwadkar, M. Yamashita, M. H. Kaplan, BATF-interacting proteins dictate specificity in Th subset activity. *J. Immunol.* **203**, 1989–1998 (2019).
 79. R. Satija, J. A. Farrell, D. Gennert, A. F. Schier, A. Regev, Spatial reconstruction of single-cell gene expression data. *Nat. Biotechnol.* **33**, 495–502 (2015).
 80. A. Butler, P. Hoffman, P. Smibert, E. Papalex, R. Satija, Integrating single-cell transcriptomic data across different conditions, technologies, and species. *Nat. Biotechnol.* **36**, 411–420 (2018).
 81. T. Stuart, A. Butler, P. Hoffman, C. Hafemeister, E. Papalex, W. M. Mauck III, Y. Hao, M. Stoeklius, P. Smibert, R. Satija, Comprehensive integration of single-cell data. *Cell* **177**, 1888–1902.e21 (2019).
 82. J. Cao, M. Spielmann, X. Qiu, X. Huang, D. M. Ibrahim, A. J. Hill, F. Zhang, S. Mundlos, L. Christiansen, F. J. Steemers, C. Trapnell, J. Shendure, The single-cell transcriptional landscape of mammalian organogenesis. *Nature* **566**, 496–502 (2019).

and AI147394). Core facility usage was also supported by Indiana University Simon Cancer Center Support grants P30 CA082709 and U54 DK106846 from the National Institutes of Health. Support provided by the Herman B Wells Center for Pediatric Research was, in part, from the Riley Children's Foundation. This project was supported by the Indiana Clinical and Translational Sciences Institute, funded in part by award number UL1TR002529 from the National Institutes of Health, National Center for Advancing Translational Sciences, and Clinical and Translational Sciences Award. This work was supported by the Brown Center for Immunotherapy. **Author contributions:** B.J.U., R.K., and M.H.K. designed the experiments. B.J.U., R.K., A.P., and T.A.H. performed the experiments. R.K., M.C., B.J.U., and H.G. performed the bioinformatic experiments and analysis. M.C., A.P., C.M., B.K., Y.F., T.A.H., and A.S.N. assisted with the experiments. H.-M. Z., N.P.G., Y.L., A.K.L., M.J.T., P.L.-L., R.A.F., and J.S. provided reagents, mice, and advice. B.J.U., R.K., and M.H.K. coordinated the project and wrote the

manuscript with input from all authors. **Competing interests:** R.A.F. is an advisor to Glaxo Smith Kline, Zai Labs, and Ventus Therapeutics. J.S. is a consultant for Teneofour. The authors declare that they have no other competing interests. **Data and materials availability:** scRNA-seq and scATAC-seq data are available under accession number GSE190795. This study did not generate any unique code. All other data needed to evaluate the conclusions in the paper are present in the paper or the Supplementary Materials.

Submitted 4 February 2021
Accepted 14 February 2022
Resubmitted 15 December 2021
Published 18 March 2022
10.1126/sciimmunol.abg9296

Allergic airway recall responses require IL-9 from resident memory CD4 T cells

Benjamin J. UlrichRakshin KharwadkarMichelle ChuAbigail PajulasCharanya MuralidharanByunghee KohYongyao FuHongyu GaoTristan A. HayesHong-Ming ZhouNick P. GoplenAndrew S. NelsonYunlong LiuAmelia K. LinnemannMatthew J. TurnerPaula Licona-LimónRichard A. FlavellJie SunMark H. Kaplan

Sci. Immunol., 7 (69), eabg9296.

Gasping over IL-9 expressing CD4s

IL-9 is involved in asthma, yet what cells it comes from and its role in seasonally induced asthma (recall immune responses) is unclear. Here, Ulrich *et al.* used an allergen rechallenge mouse model to study the impact of IL-9 producing immune cells on lung inflammation and recall responses. They found that IL-9 primarily came from multifunctional CD4 T cell resident memory (Trm) populations present in the lungs of mice. These cells secreted IL-9 in an antigen-specific manner and largely depended on IL-33 for IL-9 up-regulation. IL-9 CD4 Trm also had a unique transcriptomic and epigenetic profile compared with other T cell populations in the lung. Together, these data suggest that targeting IL-9 Trm in the lungs during seasonal allergies might abrogate lung inflammation.

View the article online

<https://www.science.org/doi/10.1126/sciimmunol.abg9296>

Permissions

<https://www.science.org/help/reprints-and-permissions>